Quantum Computational Fluid Dynamics

D. Jaksch, University of Hamburg

QCFD (qcfd-h2020.eu)

EU HORIZON-CL4-2021-DIGITAL-EMERGING-02-10
grant agreement No. 101080085 QCFD

Universität Hamburg
DER FORSCHUNG | DER LEHRE | DER BILDUNG

QSG 2025, Trento, 7th May 2025

Aerodynamic designs

- Edges reduce drags

www.nytimes.com

- Bulbous bows

www.brueckenbote.de

- Gurney flaps

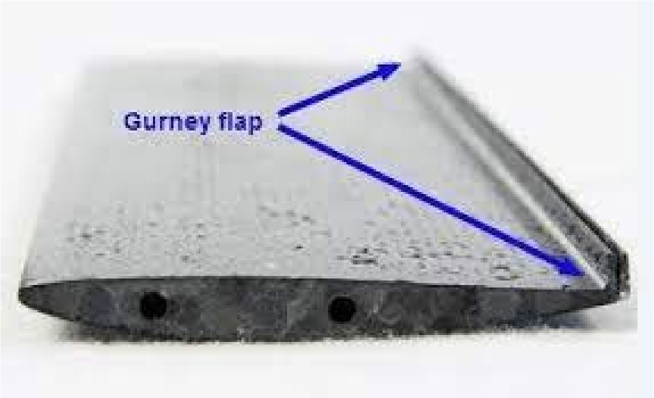

https://doi.org/10.1155/2015/402358

- Winglets

www.scienceabc.com

Kolmogorov microscale and Reynolds number

- A simulation of fluid flow needs to cover a wide range of length scales
  - L the size of the largest eddies in the flow
  - η the Kolmogorov length scale at which eddies are dissipated into heat

- The ratio of these two length scales is the Reynolds number defined as

$$\mathrm{Re} = \left(\frac{L}{\eta}\right)^{4/3} = \frac{vL}{\nu}$$

- Here v is the speed of the flow and ν the kinematic viscosity
- Flows become turbulent when Re is greater than a couple of thousands
- Grid based methods typically scale with $\mathrm{Re}^{3K/4}$

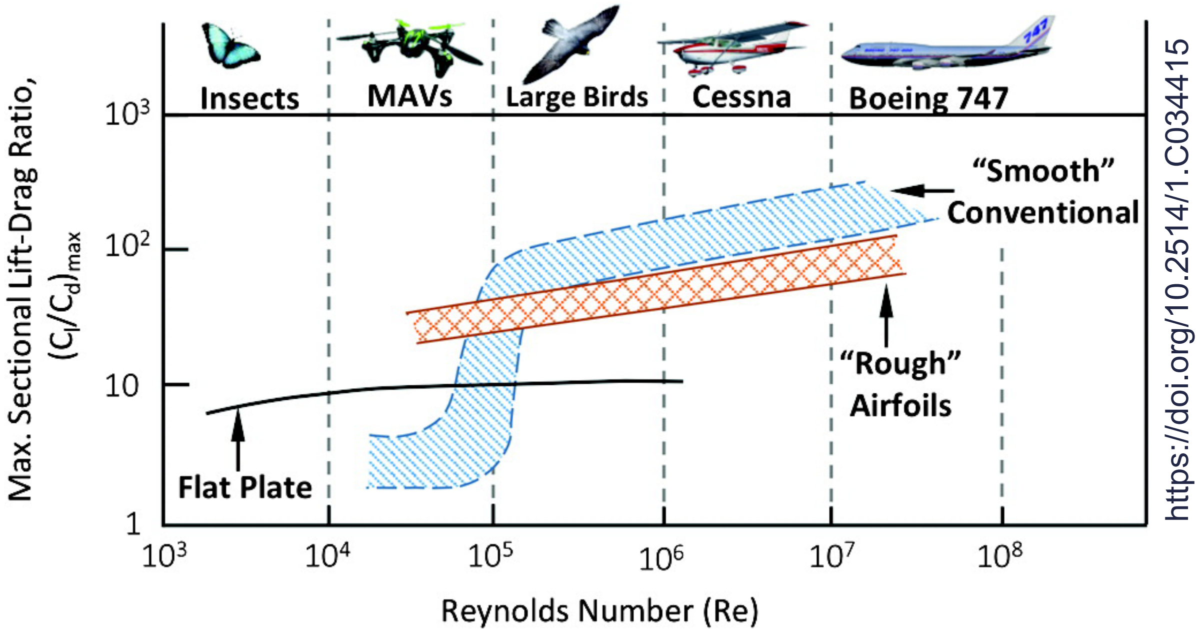

$\mathrm{Re} \approx 10^9$

$\mathrm{Re} \approx$ very large

The challenge – Resolving a wide range of length-scales

- Typically, the largest eddy size L is

$$10\text{m} \leq L \leq 100\text{m}$$

- Resolution up to the Kolmogorov length scale η, typically

$$0.1\text{mm} \leq \eta \leq 10\text{mm}$$

- Necessary Grid Points N

$$1\,000\,000\,000 \leq N \leq 1\,000\,000\,000\,000\,000\,000$$

- Necessary memory M for storing a single velocity component

$$8\text{ Mbyte} \leq M \leq 8\,000\text{ Pbyte} = 8\,000\,000\text{ Tbyte}$$

- Additionally, very small time steps are often necessary
- one usually works with approximations
  - Can work very well – especially with known configurations
  - Unfortunately, they also deliver qualitatively incorrect results

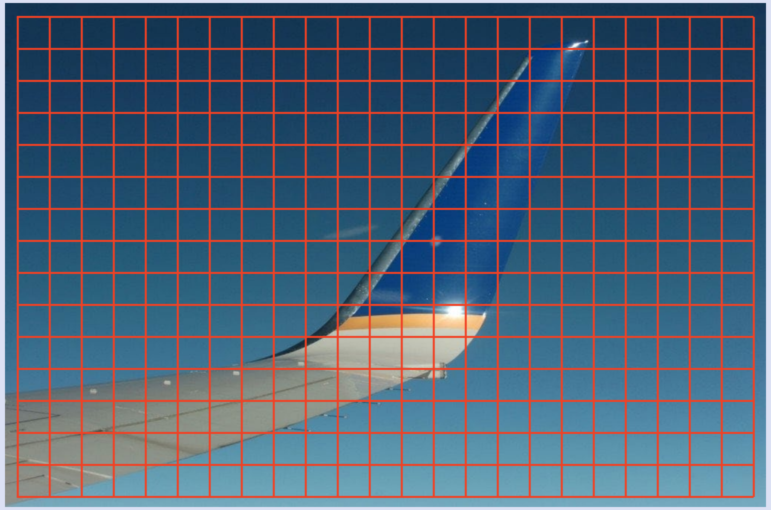

Winglets

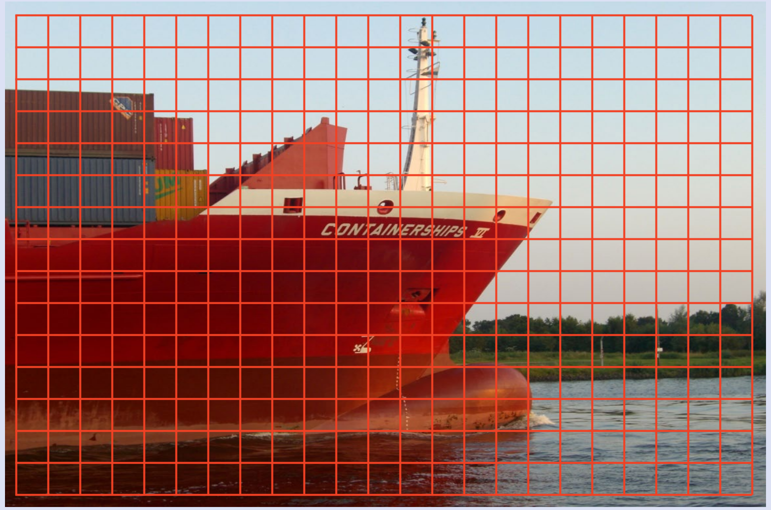

Bulbous bows

CFD Vision 2030 Research Roadmap

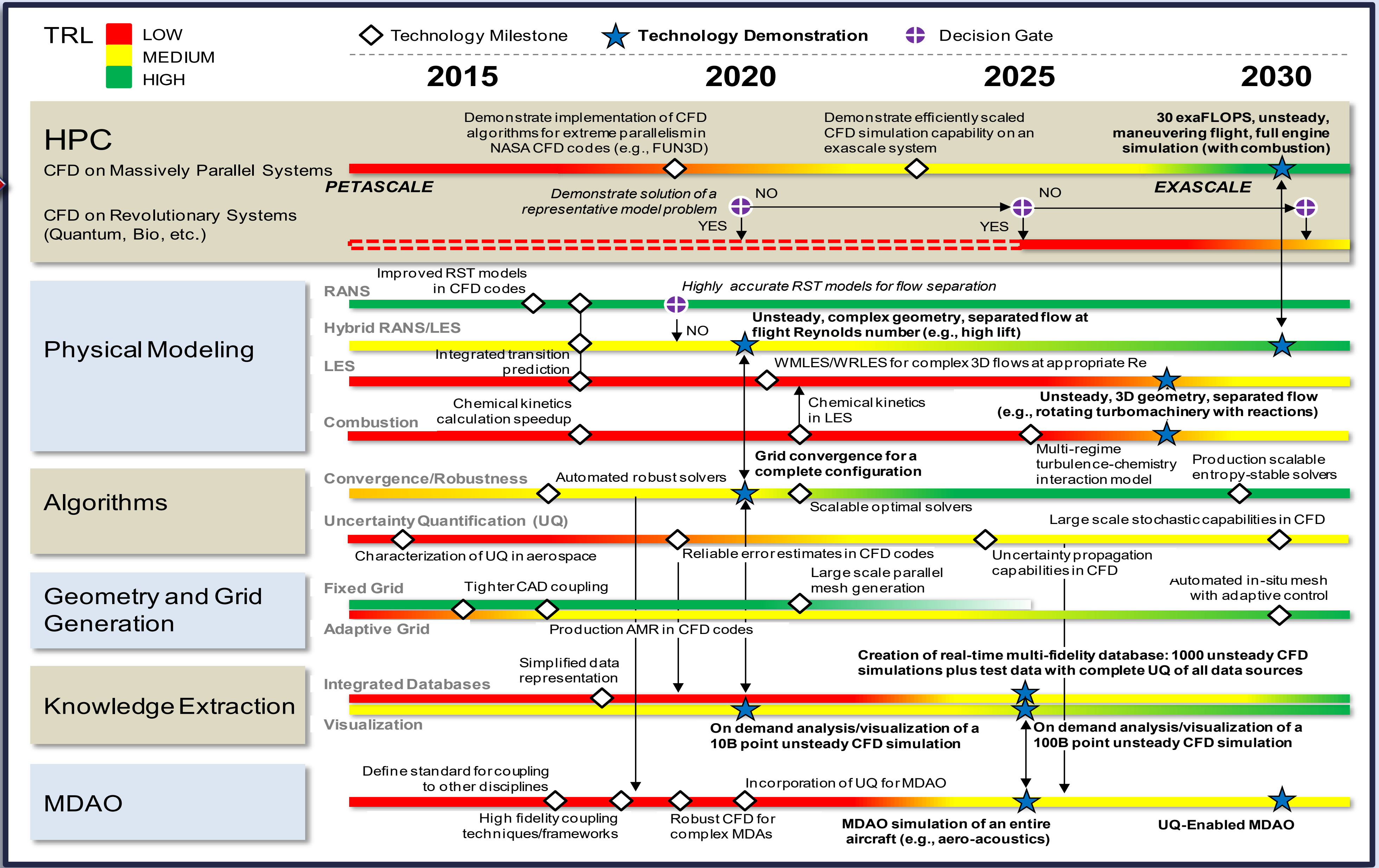

"There is steady progress on fabricating practical quantum computers, and such systems may be available in 2030. However, while a quantum computer can be used for some linear algebra calculations …, a quantum computer is not necessarily a faster computer for CFD calculations." (CFD Vision 2030 Study Report)

Incompressible Navier-Stokes equation

- We solve the 2D and 3D equations for simple fluid flows

$$\frac{\partial \vec{v}}{\partial t} = -(\vec{v} \cdot \nabla)\vec{v} - \nabla p + \frac{1}{\mathrm{Re}} \nabla^2 \vec{v}$$

$$\nabla \cdot \vec{v} = 0$$

- 2D → weather forecast
- 3D → aerodynamics, combustion physics, …

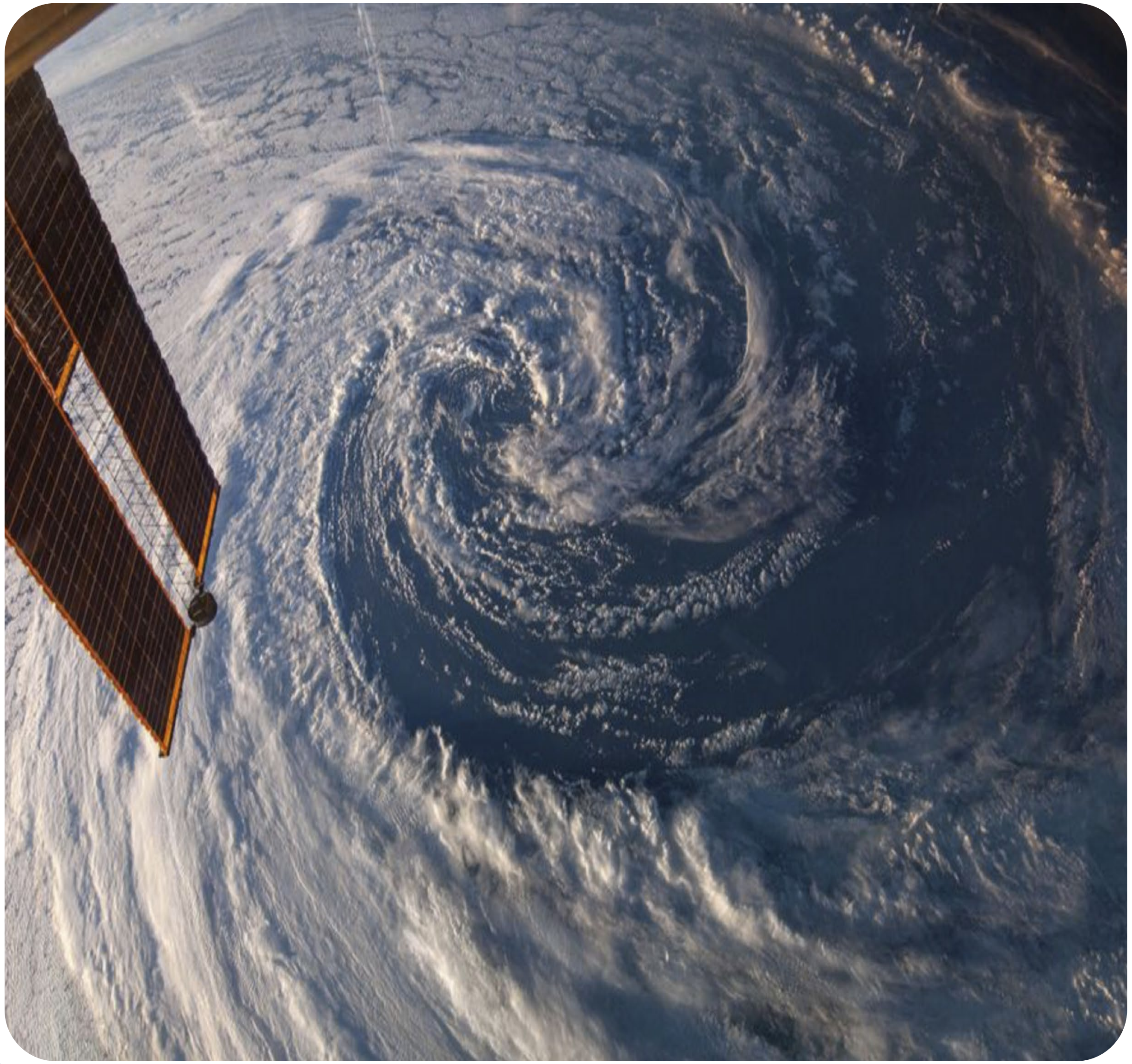

The energy cascade – two and three spatial dimensions

- Richardson in 1922 on 3D turbulence:

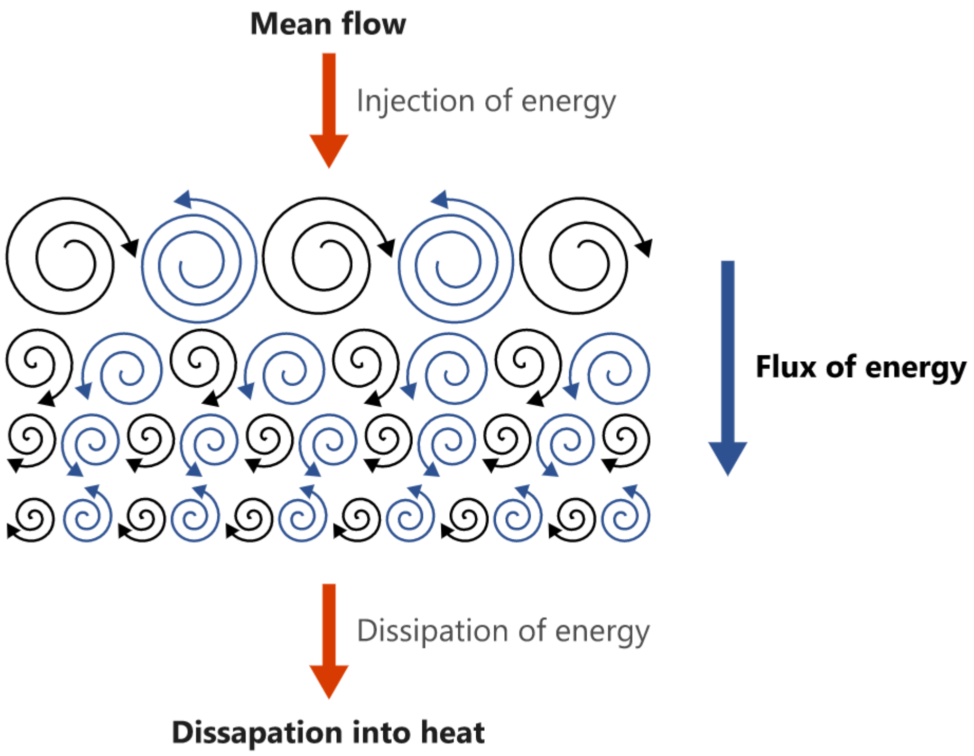

3D

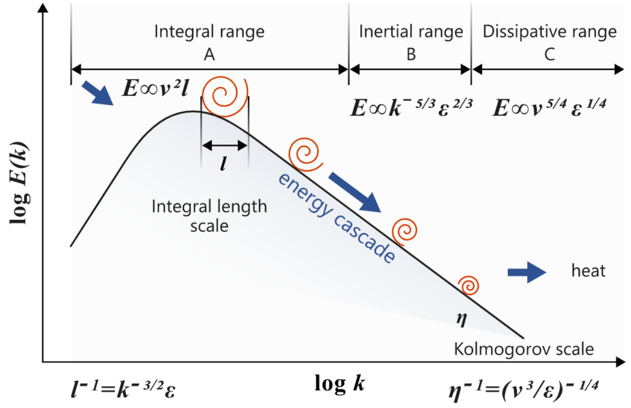

altair.com

2D

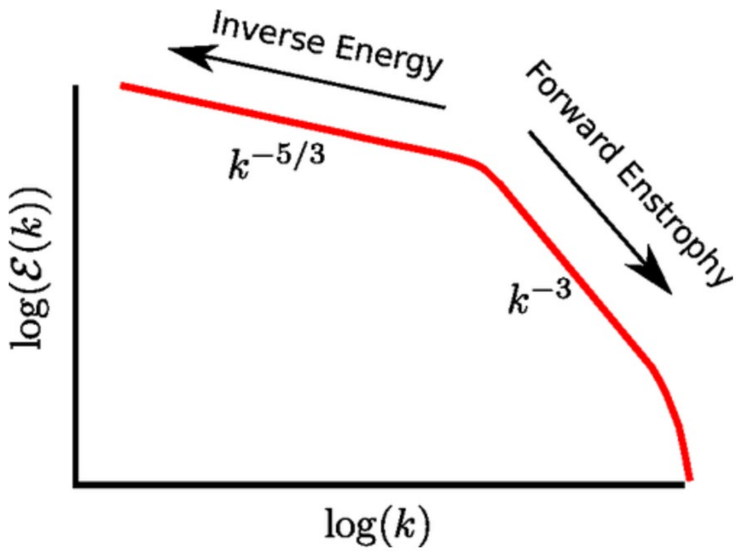

www-vortex.mcs.st-and.ac.uk/

Outline

MPS

- Encoding grid functions
- Classical entanglement spectrum
- Turbulence correlations

CFD Examples

- MPS algorithm
- Jet formation
- Taylor Green vortex
- Driven cavity

Hybrid Optimization

- Hardware architecture
- Quantum network
- Generic cost function
- Proof of Principle Example

MPS – Classical Entanglement Spectra

- Consider a scalar field $u(\boldsymbol{r}_q)$ on a $2^N \times 2^N$ of size $L \times L$.
- We decompose the field into functions on a coarse $L/2$ grid (red dots $\boldsymbol{X}_k$) and a fine grid (black dots) as

$$u(\boldsymbol{r}_q) = \sum_{\alpha=1}^{\chi(1)} \lambda_\alpha R_\alpha(\boldsymbol{X}_k) f_\alpha(\boldsymbol{x}_l) \quad \text{where} \quad \mathbf{r}_\mathrm{q} = \mathbf{X}_\mathrm{k} + \mathbf{x}_\mathrm{l}$$

- The maximum number of terms in this sum is

$$\chi_{\max}(1) = 4$$

- The actually required number of terms $\chi(1)$ in this sum is the so-called Schmidt number. It is a measure of correlations between $L/2$ and other length scales.
- The terms in the sum are weighted by λ_α which is the entanglement spectrum.

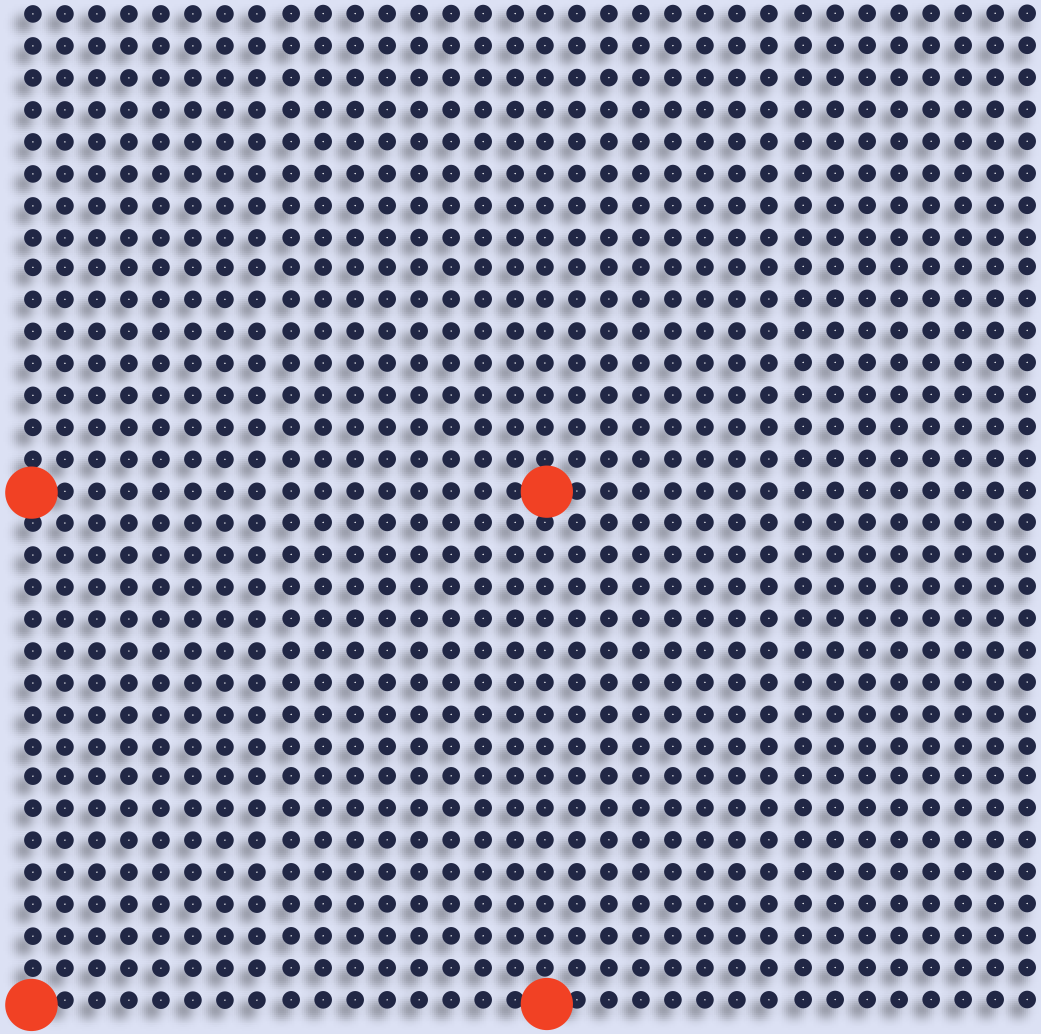

MPS – Encoding Grid Functions

- We encode the grid positions into basis states of two qubits

$$|00\rangle \qquad |01\rangle \qquad |10\rangle \qquad |11\rangle$$

- The function values are basis state amplitudes

$$|f_\alpha\rangle = R_\alpha(\boldsymbol{X_{00}})|00\rangle + R_\alpha(\boldsymbol{X_{01}})|01\rangle + R_\alpha(\boldsymbol{X_{10}})|10\rangle + R_\alpha(\boldsymbol{X_{11}})|11\rangle$$

- The 2 qubit state may be entangled, so all required R_α can be encoded into just 2 qubits.

$$|\psi\rangle = \sum_\alpha \lambda_\alpha |f_\alpha\rangle \otimes |\phi_\alpha\rangle$$

- Here, $|\phi_\alpha\rangle$ will be used to encode the rest of the function.

Note: For the whole grid only $2N$ qubits are required

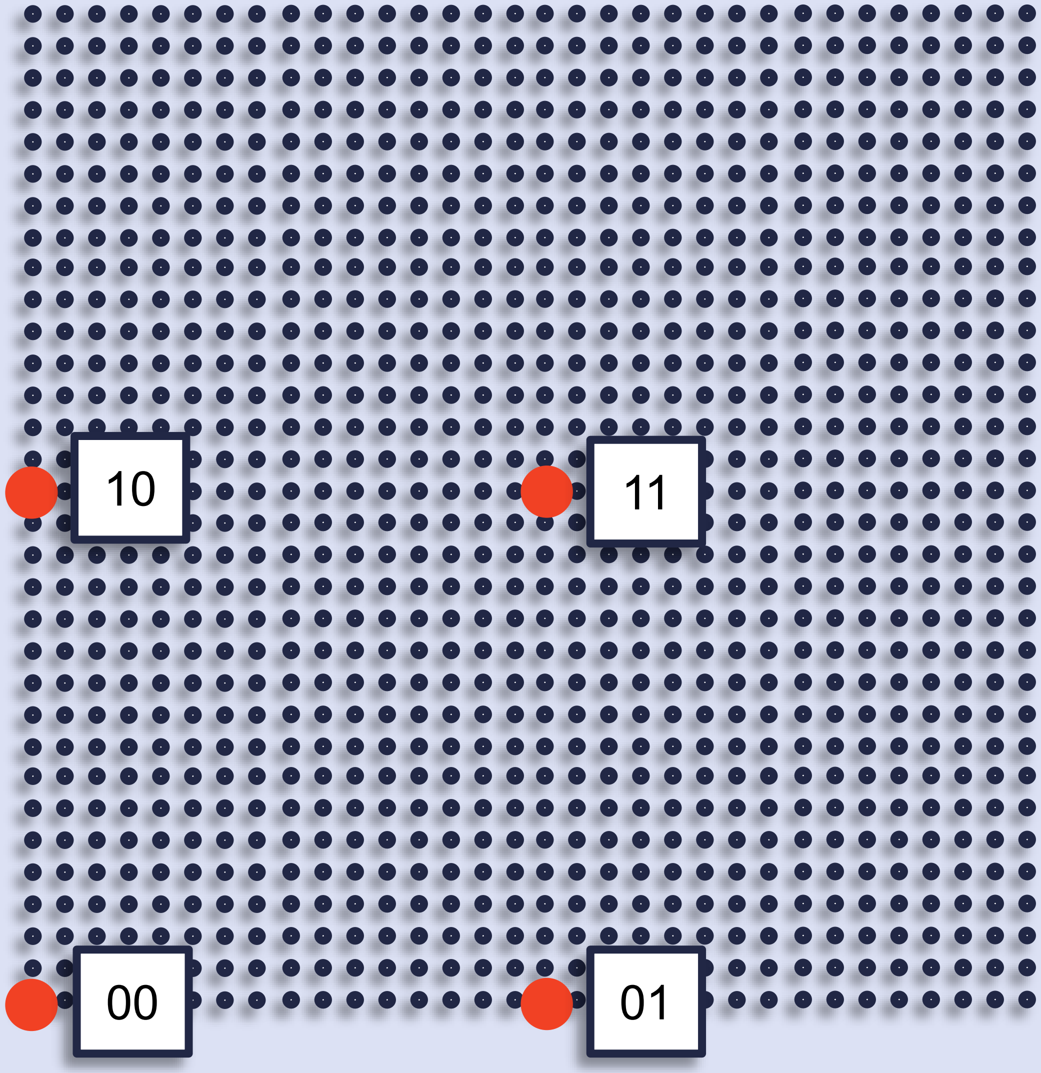

MPS – Classical Entanglement Spectra

- We repeat this decomposition to get correlations between neighbouring length scales.
- For instance, for correlations between the length scale $L/4$ and lengths scale $L/8$ we decompose each of the functions $f_\alpha(x_l)$ from before.
- This gives a representation of the field as

$$u = \sum_{\alpha=1}^{\chi(1)} \lambda_\alpha R_\alpha \sum_{\beta=1}^{\nu} \lambda_\beta R_{\alpha\beta} f_{\alpha\beta}$$

- The maximum Schmidt number $\chi(2)$ is the total number of terms in these sums

$$\chi_{\max}(2) = 4^2 = 16$$

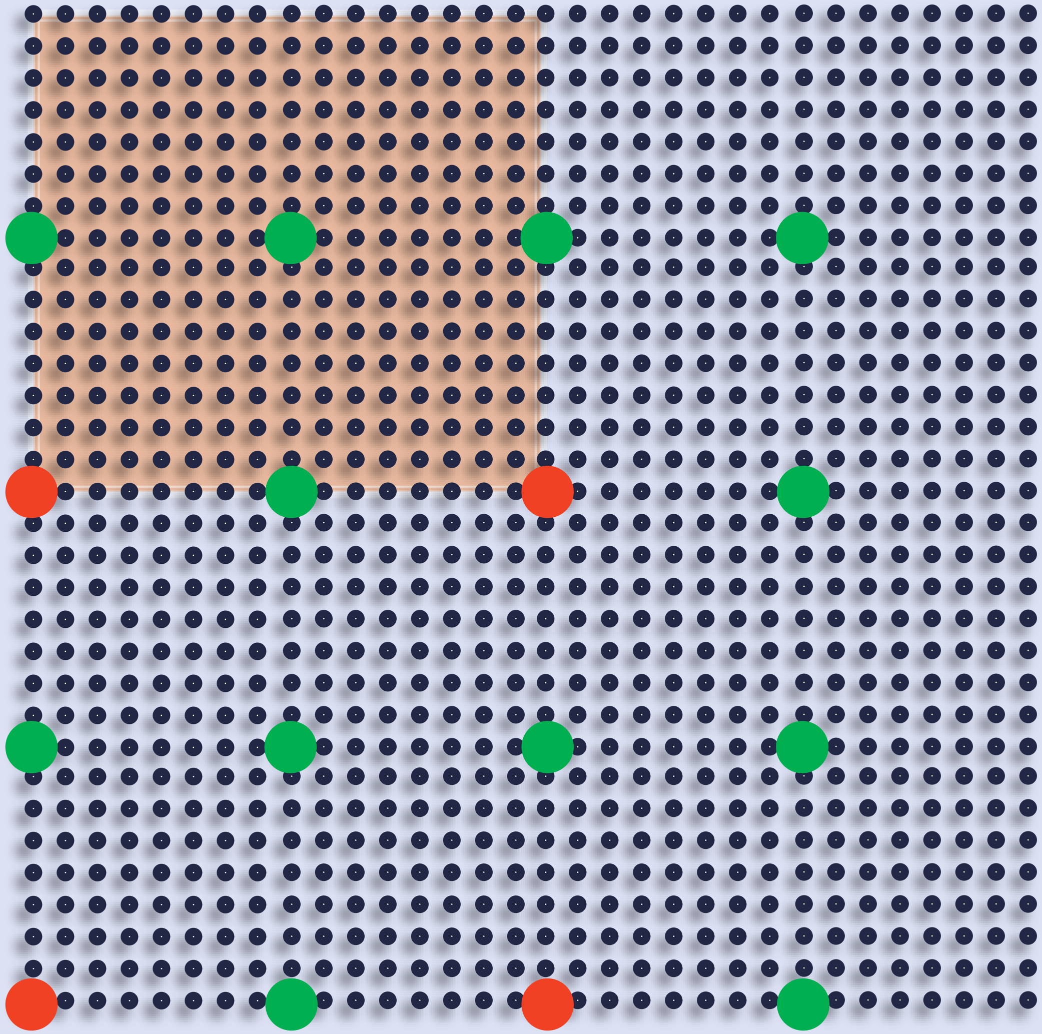

MPS – Classical Entanglement Spectra

- In general, Schmidt numbers $\chi(n)$ and $\lambda_\alpha^{(n)}$ characterize the amount of correlations between length scales

$$L \times 2^{-n} \quad \text{and} \quad L \times 2^{-n-1}$$

- The repeated application of Schmidt decompositions with increasing n gives a compact Matrix-Product-State (MPS) representation of the scalar field

$$u(\boldsymbol{r_q}) = A^{q_1} A^{q_2} A^{q_3} A^{q_4} \cdots A^{q_N}$$

- Here A^{q_i} is a $\chi(i-1) \times \chi(i)$ matrix.
- The index q_i labels the position in the i-th 2×2 sub-grid $00, 01, 10, 11$.
- In principle the maximum χ can grow exponentially with the fineness of the grid.

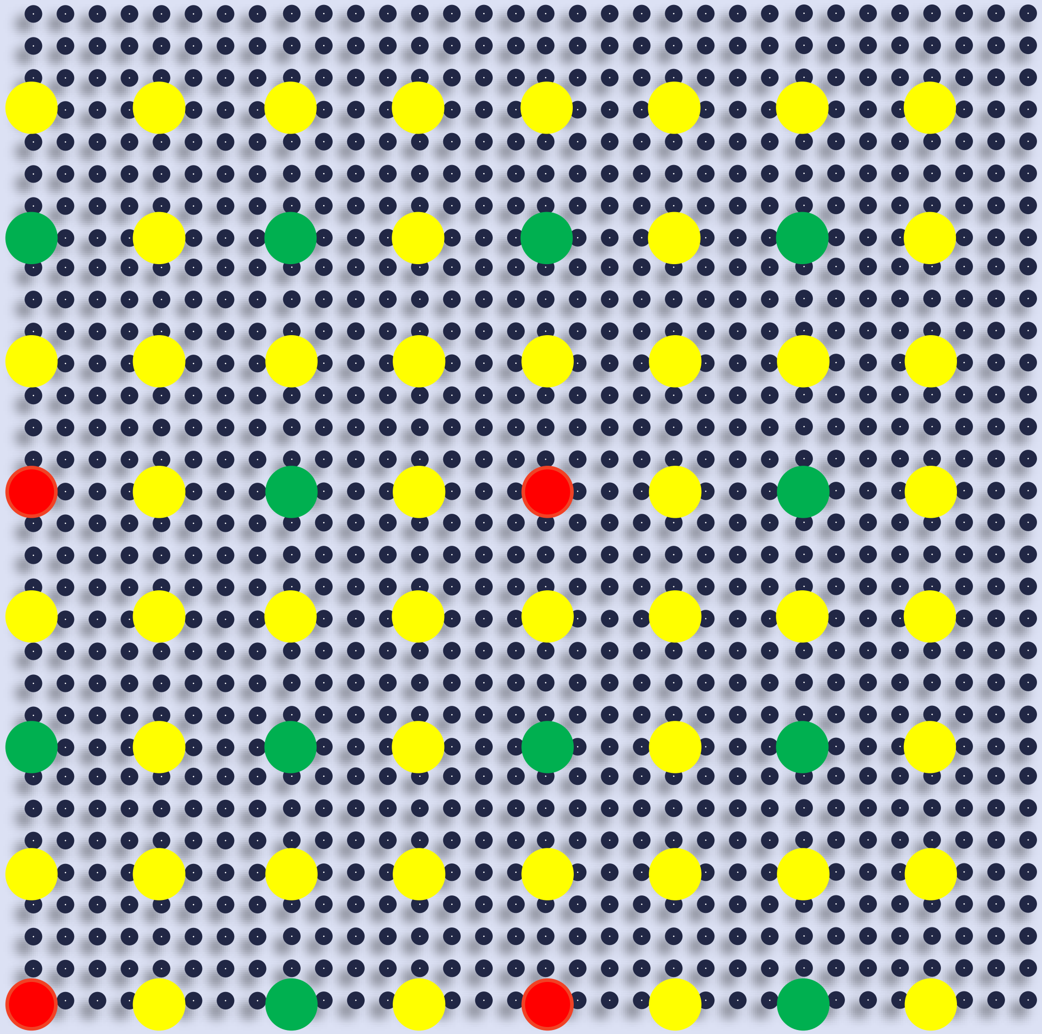

MPS – Turbulence Correlations

N. Gourianov, et al., Nature Computational Science **2**, 30 (2022).

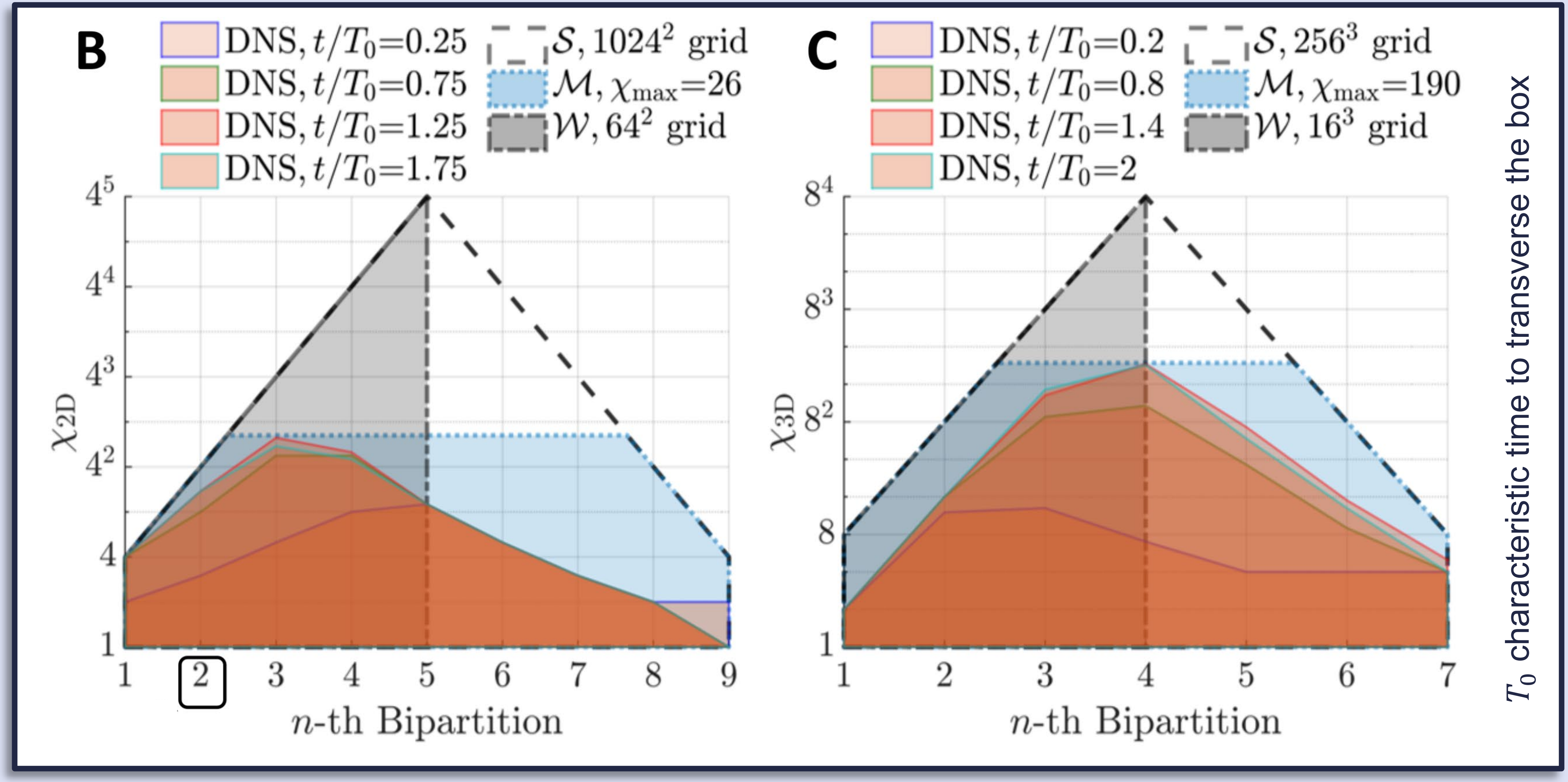

T_0 characteristic time to transverse the box

2D developing jet, Re=1000

3D Taylor-Green vortex, Re=800

Entanglement entropy

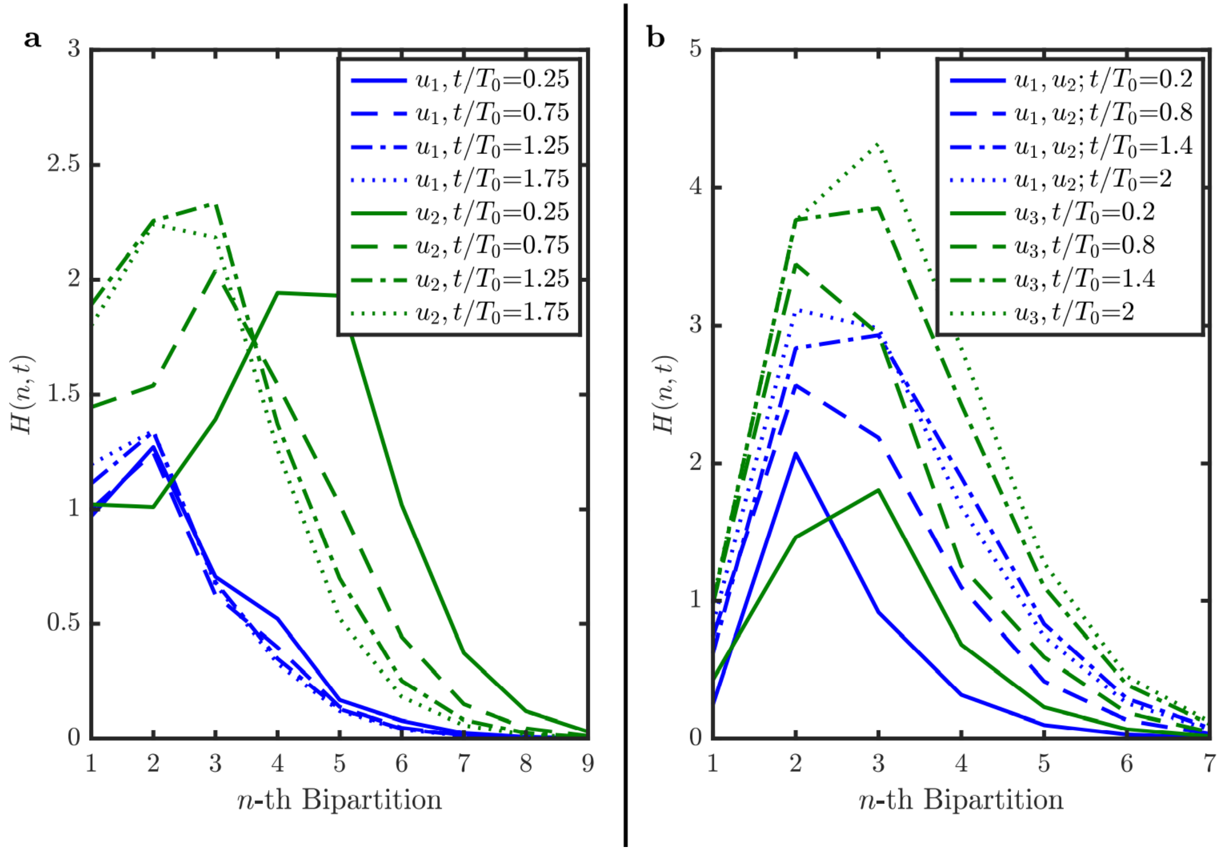

2D developing jet, Re=1000

3D Taylor-Green vortex, Re=800

- The entanglement entropy is different for 2D and 3D flows
- For 2D the entropy shifts to coarser length scales with increasing time, consistent with the inverse energy cascade
- In 3D the opposite happens consistent with energy cascade energising small length scales.

Outline

MPS

- Encoding grid functions
- Classical entanglement spectrum
- Turbulence correlations

CFD Examples

- MPS algorithm
- Jet formation
- Taylor Green vortex
- Driven cavity

Hybrid Optimization

- Hardware architecture
- Quantum network
- Generic cost function
- Proof of Principle Example

MPS algorithm for evolving a 2D fluid flow in time

- We illustrate this by considering a simple Euler step to move forward in time by Δt.
- For this we minimize the cost function

$$\Theta(\vec{v}^*) = \mu|\overline{\nabla}\cdot\vec{v}^*|^2 + \left|\frac{\vec{v}^* - \vec{v}}{\Delta t} + (\vec{v}\cdot\overline{\nabla})\vec{v} - \nu\overline{\nabla}^2\vec{v}\right|^2$$

- We use eighth-order central finite difference stencils and represent the Laplace operator as an MPO.
- We write out explicitly $\vec{v} = u_1\vec{e}_1 + u_2\vec{e}_2$ and $\vec{v}^* = u_1^*\vec{e}_1 + u_2^*\vec{e}_2$ and write the components as bold vectors on the grid, e.g. $\boldsymbol{u}_1 = \{u_1(r_1), u_1(r_1)\cdots\}$ and rewrite the cost function as

$$\Theta(\boldsymbol{V}^*) = \sum_{i,j=1}^{2}\left\{\mu\left(\frac{\Delta\boldsymbol{u}_i^*}{\Delta x_i}\right)^t\frac{\Delta\boldsymbol{u}_j^*}{\Delta x_j}\right\} + \sum_{i=1}^{2}\left\{\frac{(\boldsymbol{u}_i^*)^t\boldsymbol{u}_i^*}{\Delta t^2} + \frac{(\boldsymbol{u}_i^*)^t}{\Delta t}\left(\frac{-\boldsymbol{u}_i}{\Delta t} + \sum_{j=1}^{2}\left\{\boldsymbol{u}_j\frac{\Delta\boldsymbol{u}_i}{\Delta x_j} - \nu\frac{\Delta^2\boldsymbol{u}_i}{\Delta x_j^2}\right\}\right)\right.$$
$$\left. + \left(\frac{-\boldsymbol{u}_i}{\Delta t} + \sum_{j=1}^{2}\left\{\boldsymbol{u}_j\frac{\Delta\boldsymbol{u}_i}{\Delta x_j} - \nu\frac{\Delta^2\boldsymbol{u}_i}{\Delta x_j^2}\right\}\right)^t\frac{\boldsymbol{u}_i^*}{\Delta t}\right\} + [\ldots],$$

- The terms in $[\cdots]$ are constant and thus irrelevant for the optimization, a step scales like $\mathcal{O}(N\chi^4)$ or $\mathcal{O}(\chi^4\log L)$.

CFD Examples – Jet Formation

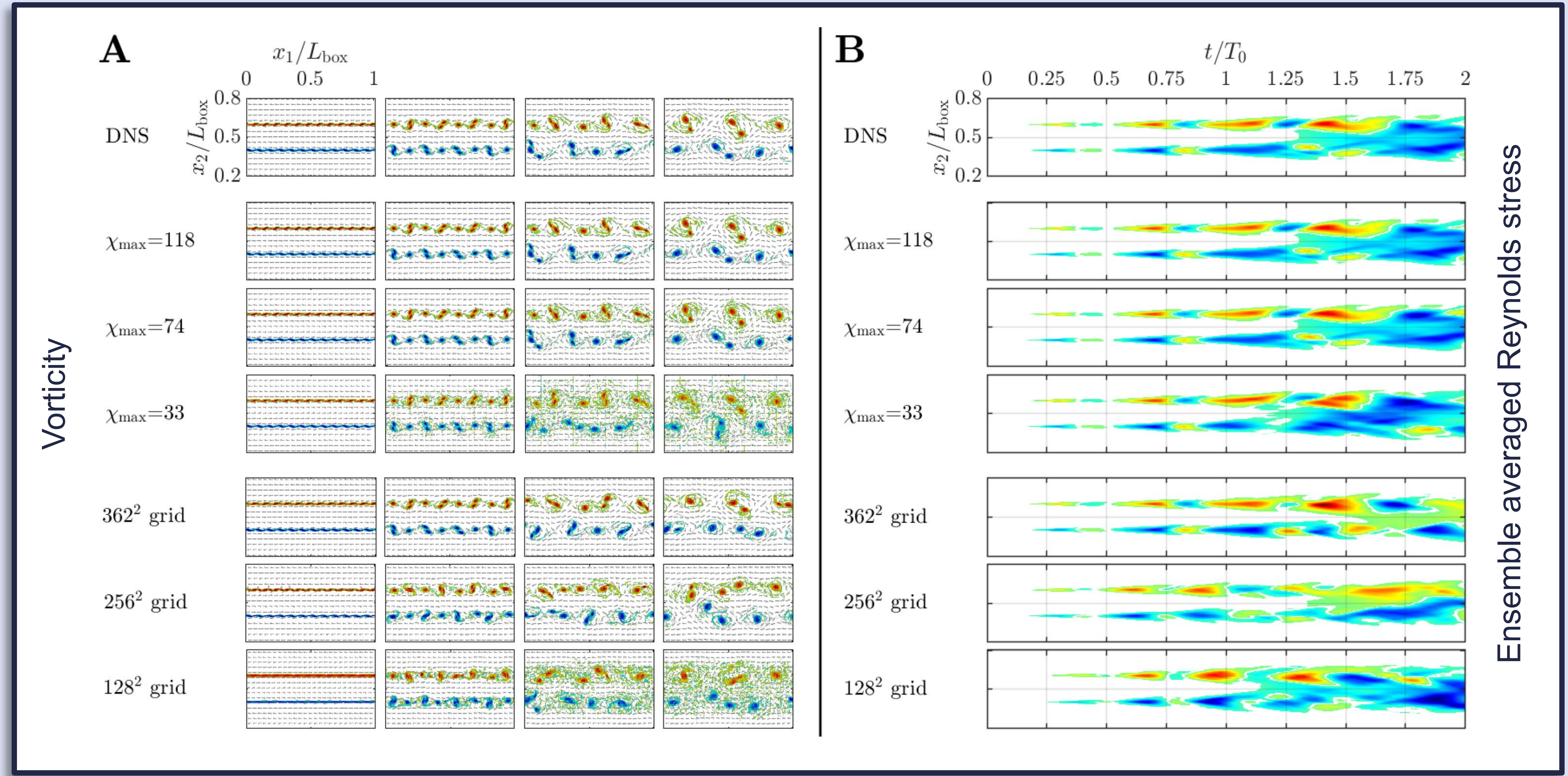

CFD Examples – Jet Formation

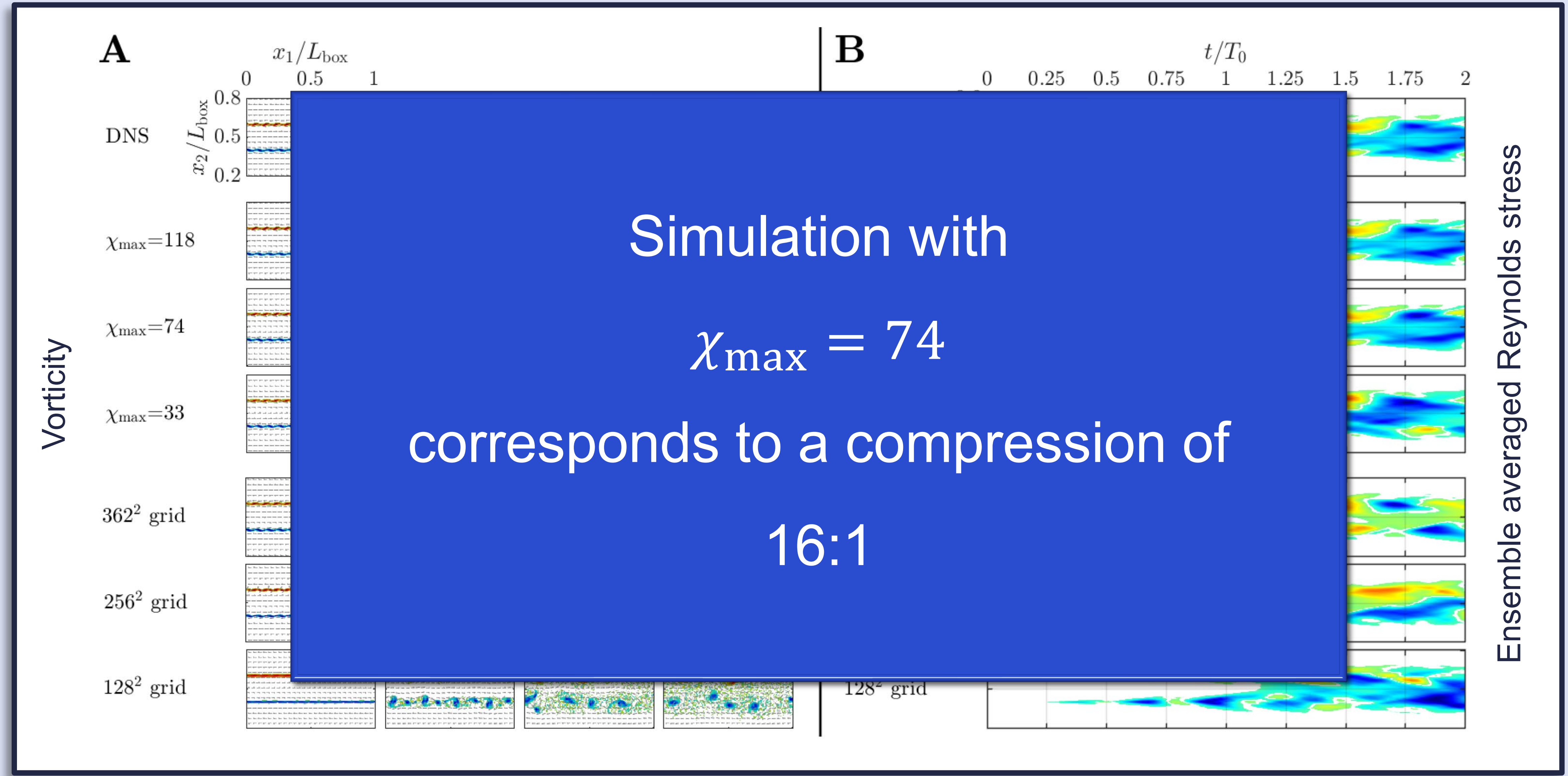

Simulation with

$$\chi_{\max} = 74$$

corresponds to a compression of

16:1

CFD Examples – Taylor Green Vortex

Vortical structures at $t = 0.2T_0, 1.4T_0, 2T_0$

(rendered using the λ_2 method)

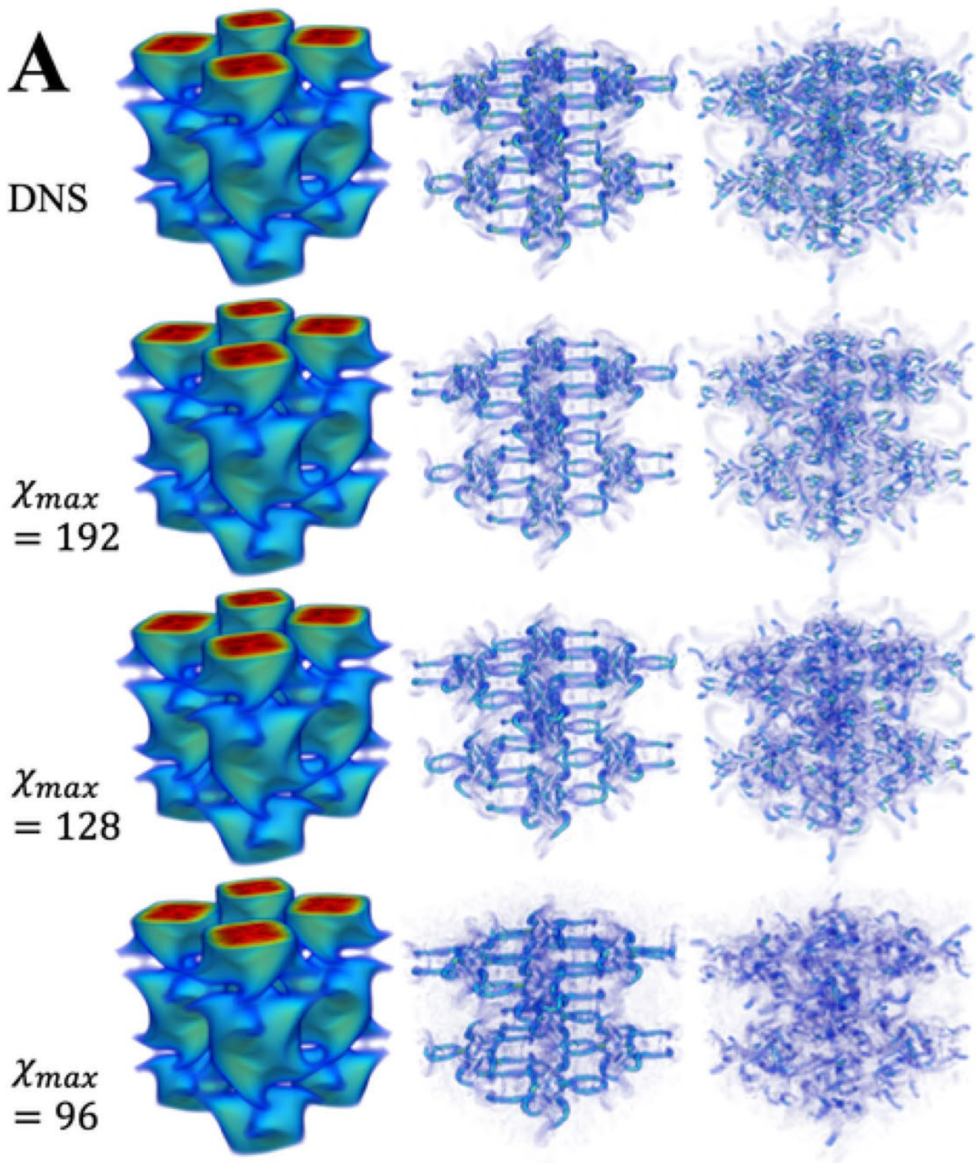

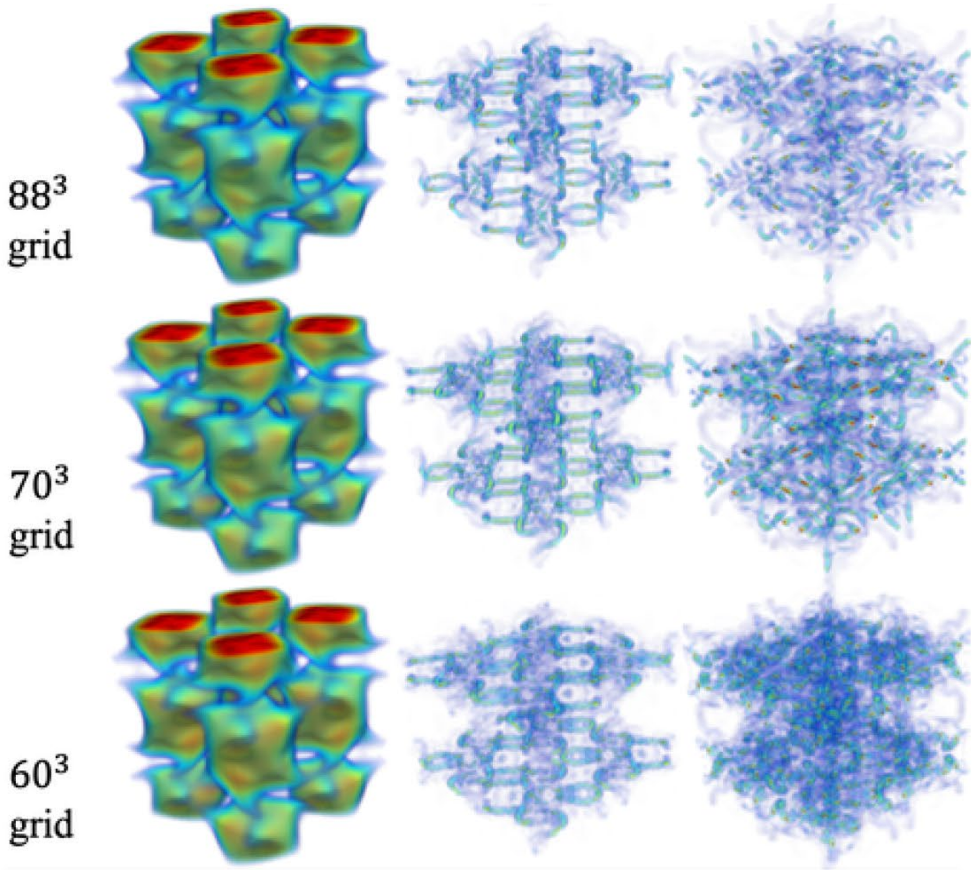

CFD Examples – Taylor Green Vortex

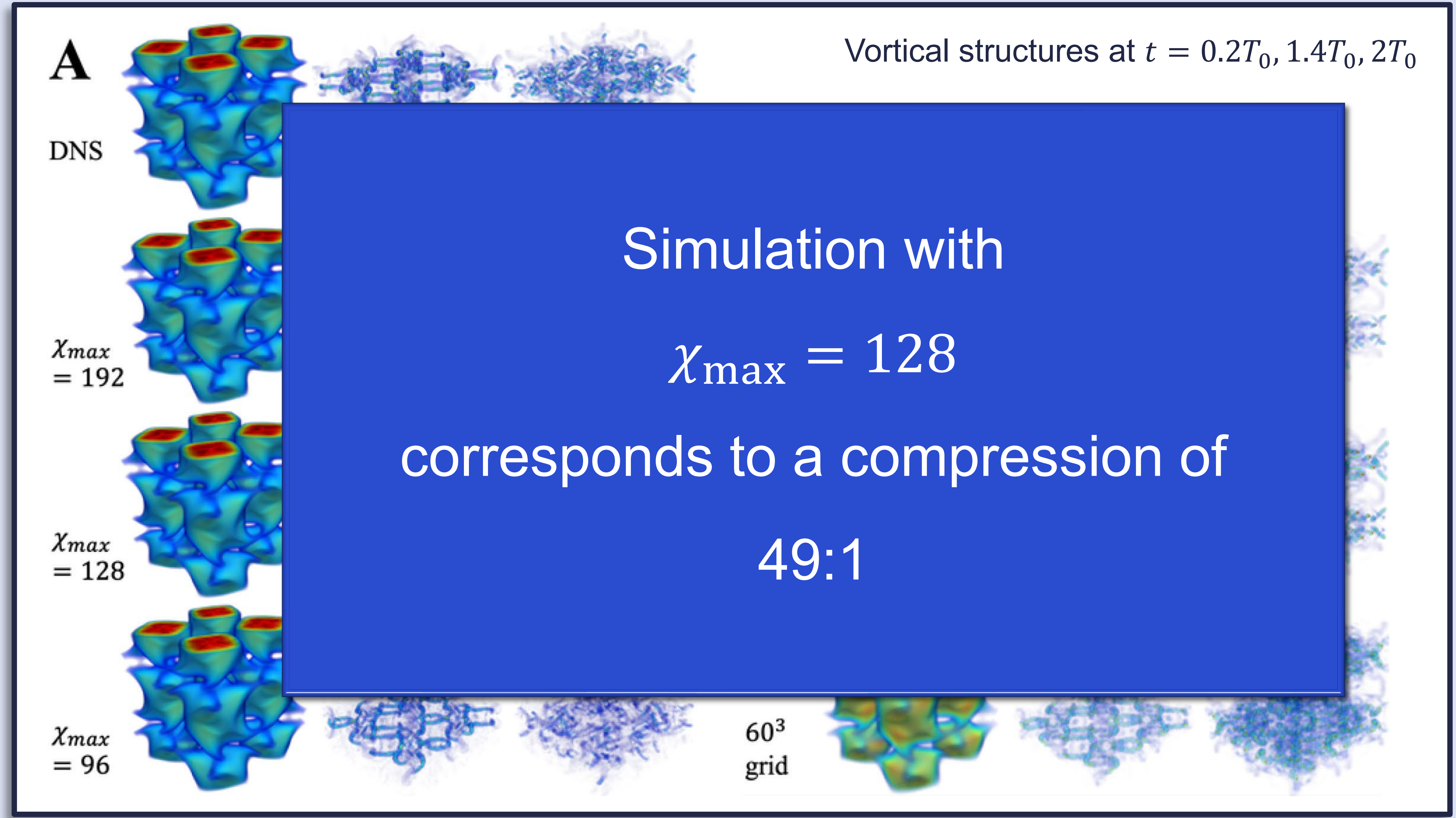

Vortical structures at $t = 0.2T_0, 1.4T_0, 2T_0$

Simulation with

$\chi_{\max} = 128$

corresponds to a compression of

49:1

Gaining a computational advantage in runtime?

- Scaling is often assessed as a function of characteristic numbers like the Reynolds number

$$Re = \left(\frac{L}{\eta}\right)^{4/3}$$

- Here L is the largest size of the energy containing eddies and η is the Kolmogorov microscale.

- Typically, numerically exact methods are expected to scale like $Re^{3K/4}$ where K is the number of spatial dimensions.

- The runtime scales as $\mathrm{Re}^{4\chi_{99}}$ which means favourable scaling for TDJ with $K = 2$ where $\chi_{99} \approx const.$ but not for the TGV with $K = 3$ where $\chi_{99} \approx 0.71$ for the two examples studied above.

- **Note:** we do not know the general scaling.

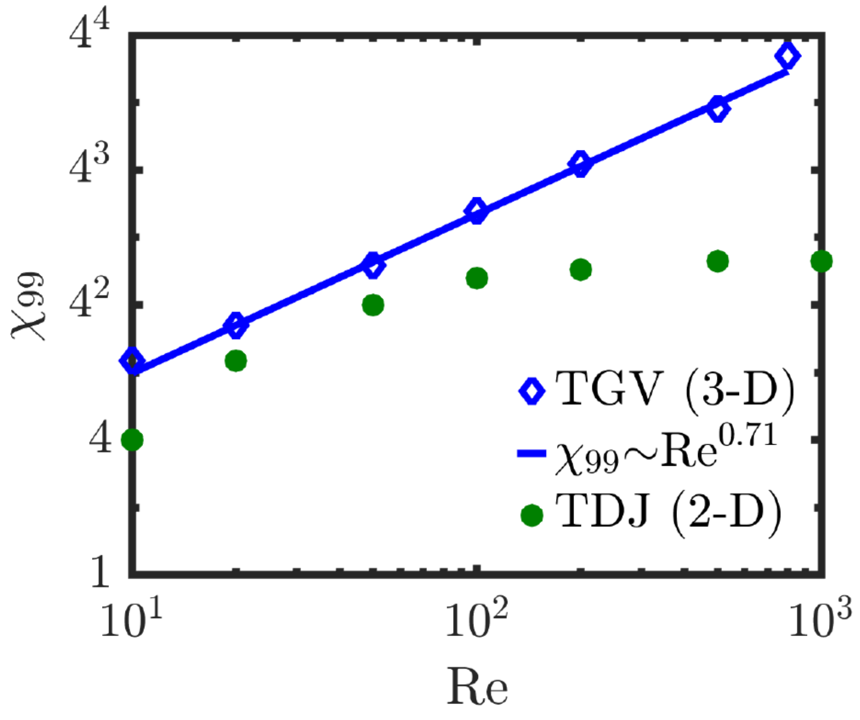

Schmidt number χ_{99} required for a 99% accurate representation of a flow field. The blue diamonds are for a decaying TGV in 3D where $\chi_{99} \propto Re^{0.71}$ for sufficiently large Re. The green dots arise from a 2D TDJ. Here $\chi_{99} \propto Re^0$ for sufficiently large Re.

Incompressible flow – boundary conditions

- Time evolution starting from the fluid and the lid at rest.

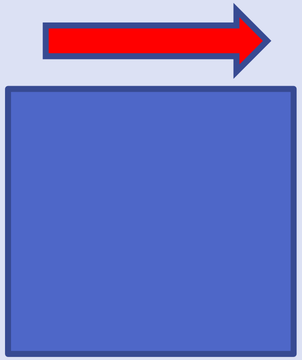

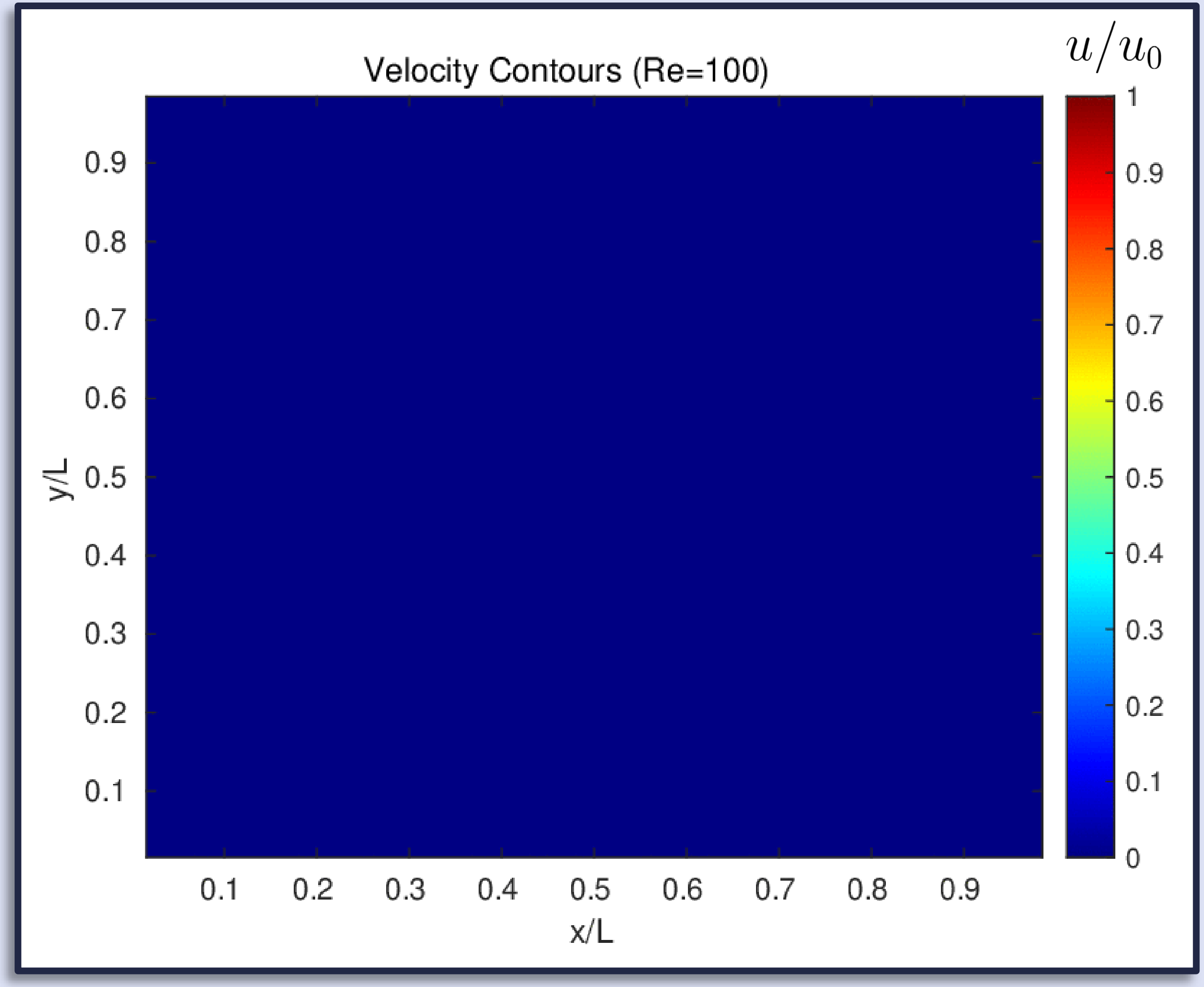

W. Y. Soh and J. W. Goodrich, Journal of Computational Physics **79**, 113 (1988).

Tensor Network CFD algorithms

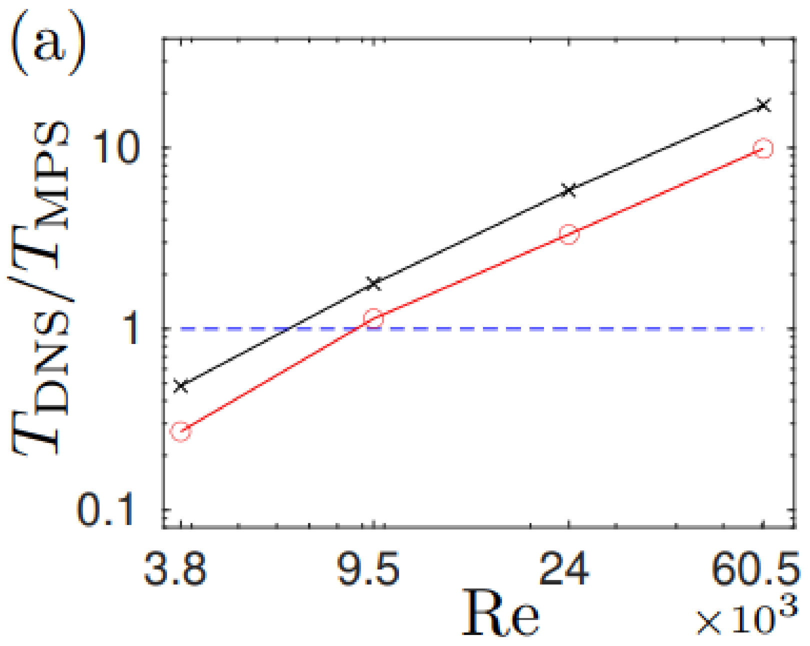

- Black: only top lid moves
- Red: top and bottom lid move

Operation	Algorithm	Scaling
Addition	Variational addition of MPS (see Sec. 4.5 in [10]).	χ^3
Multiplication	Multiplication algorithm in [22] combined with variational compression [10] of the product MPS.	$\chi^4 \rightarrow \chi^3$
Poisson solver	MPS algorithm for solving the Poisson equation in [23].	χ^3
Matrix-vector multiplication	MPO-MPS contraction combined with variational compression (see Sec. 5 in [10]). For the system considered here, the MPO bond dimension $D \leq 6$ and thus $D \ll \chi$.	$D\chi^3$

M. Kiffner and DJ, *Tensor network reduced order models for wall-bounded flows*, Phys. Rev. Fluids **8**, 124101 (2023).

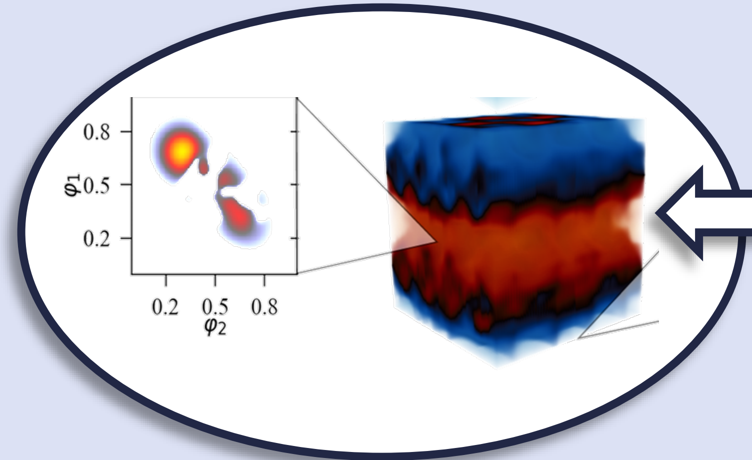

Sci. Adv. **11**, eads5990 (2025)

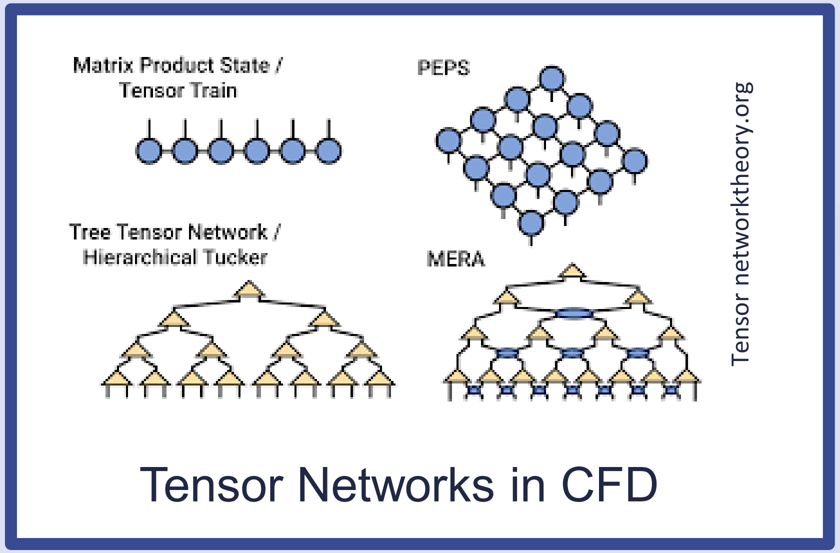

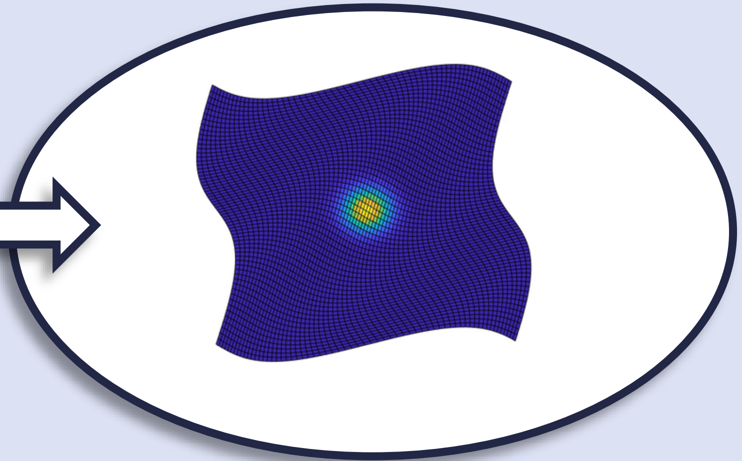

N.-L. van Hülst et al. in preparation

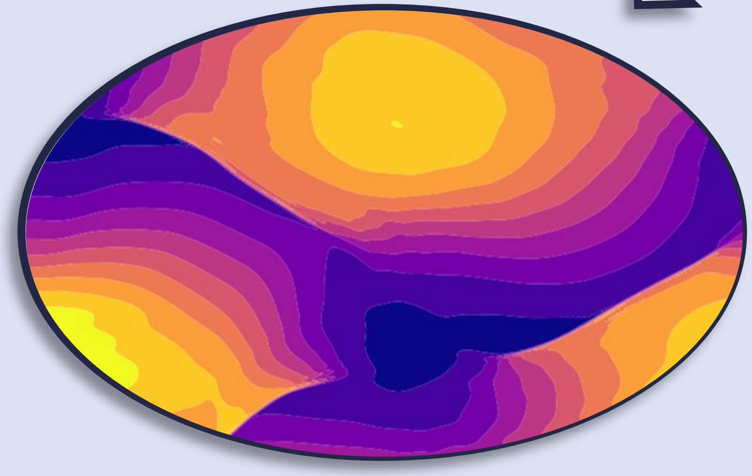

R. Pinkston et al., in preparation

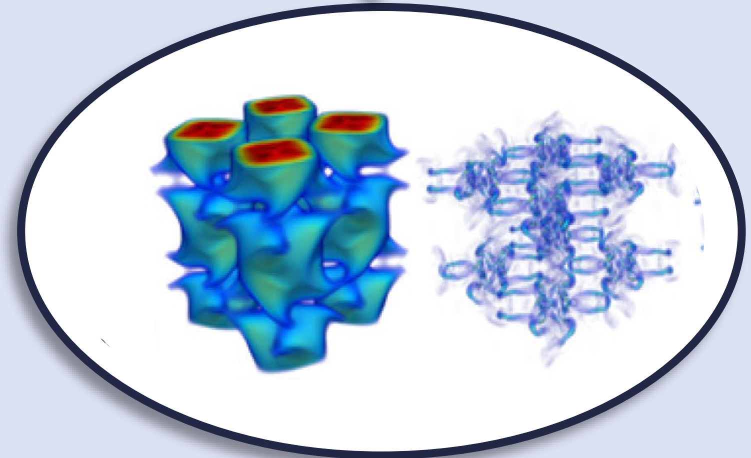

Nature Comp. Science **2**, 30 (2022).

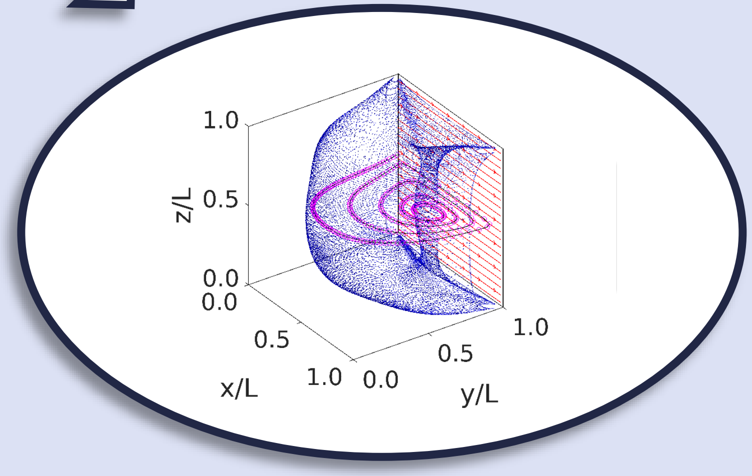

Phys. Rev. Fluids **8**, 124101 (2023)

Outline

MPS

- Encoding grid functions
- Classical entanglement spectrum
- Turbulence correlations

CFD Examples

- Jet formation
- Taylor Green vortex
- Driven cavity

Hybrid Optimization

- Hardware architecture
- Quantum network
- Generic cost function
- Proof of Principle Example

Hybrid Optimization – Hardware Architecture

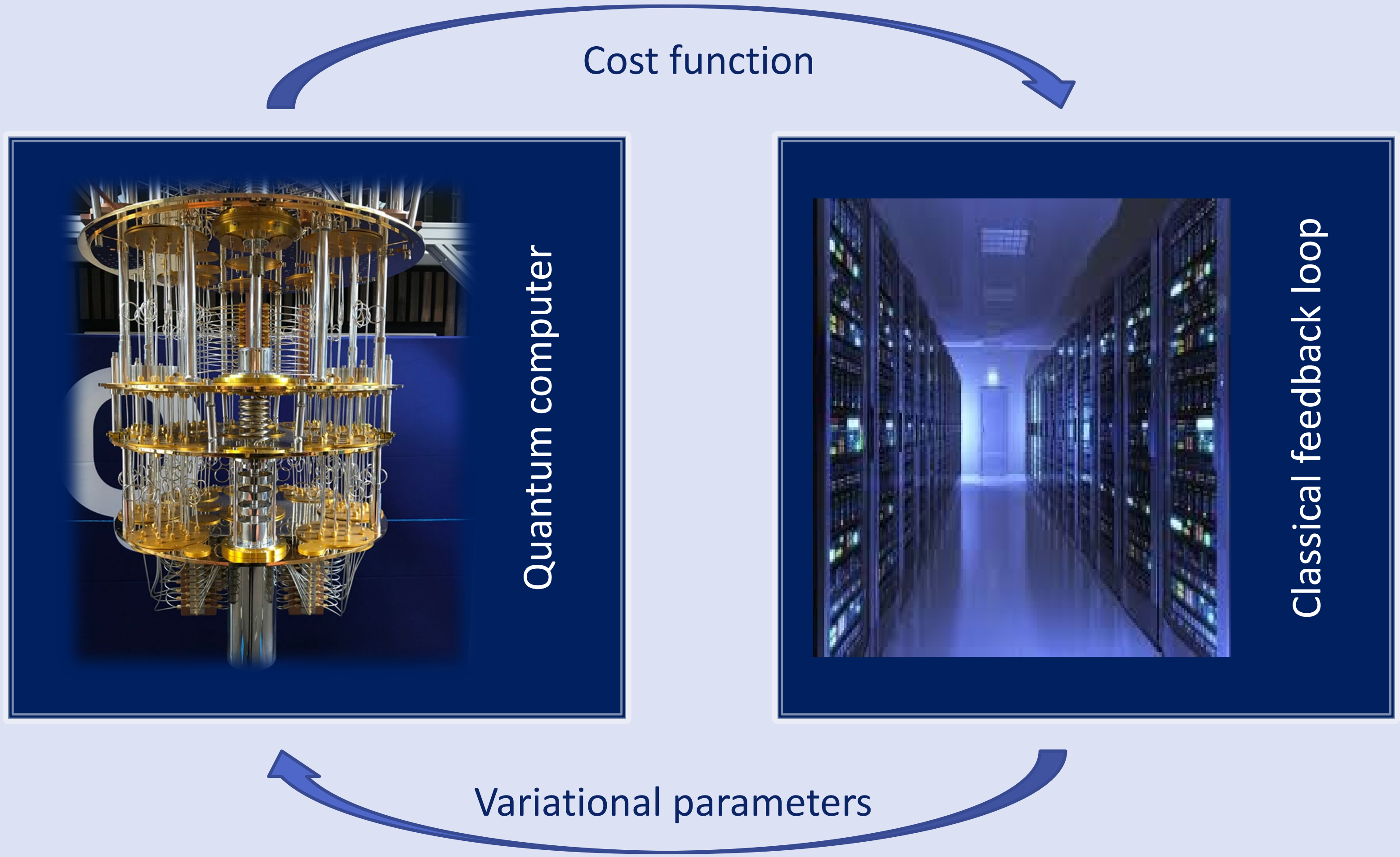

A. Peruzzo, et al., Nat. Commun. **5**, 4213 (2014).

Hybrid Optimization – Hardware Architecture

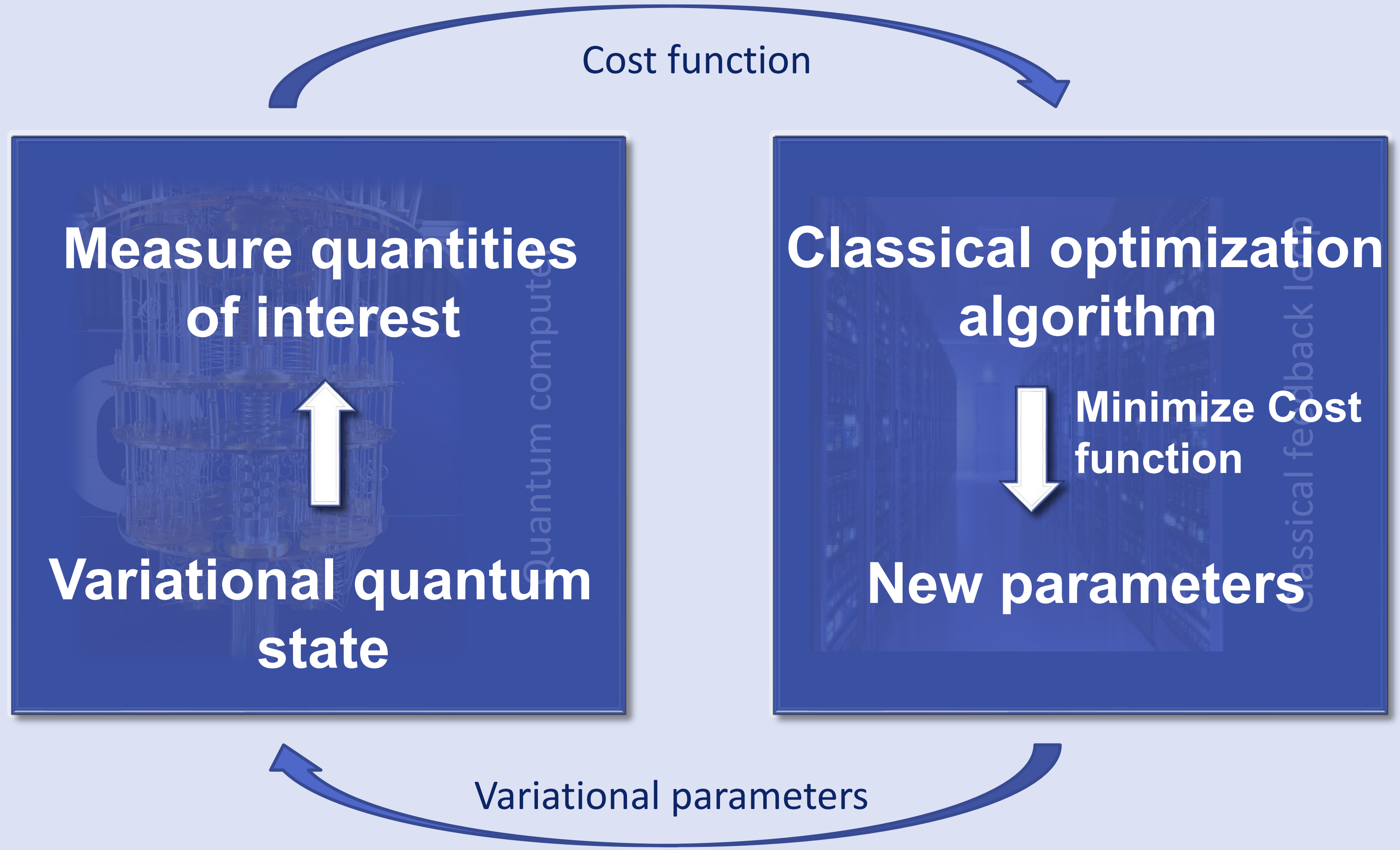

A. Peruzzo, et al., Nat. Commun. **5**, 4213 (2014).

Hybrid Optimization – Hardware Architecture

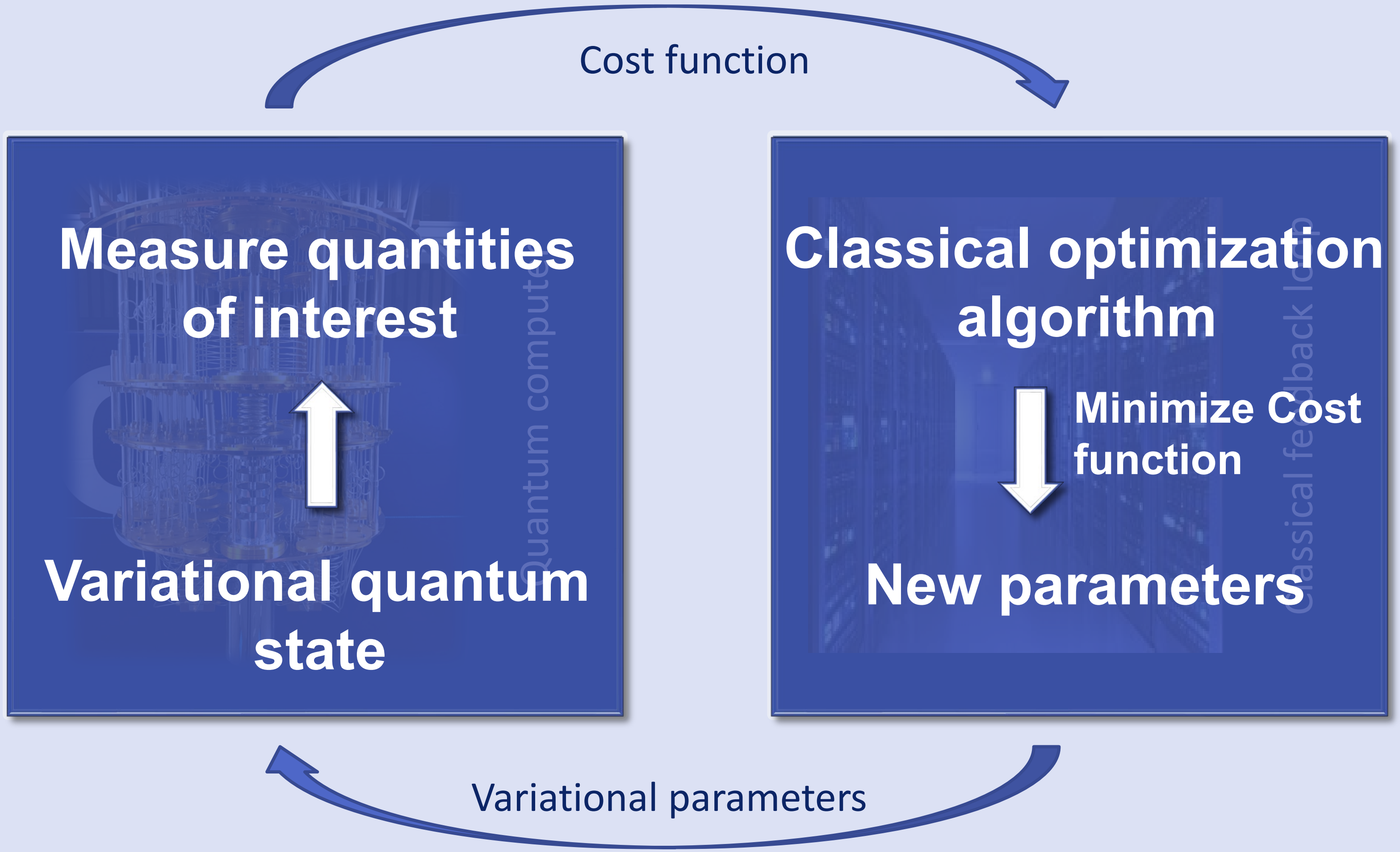

Our work: Extension to **nonlinear** problems

M. Lubasch, J. Joo, P. Moinier, M. Kiffner & DJ, Phys. Rev. A **101**, 010301(R) (2020).

The QNPU Quantum Network for cost function $\mathcal{C}$

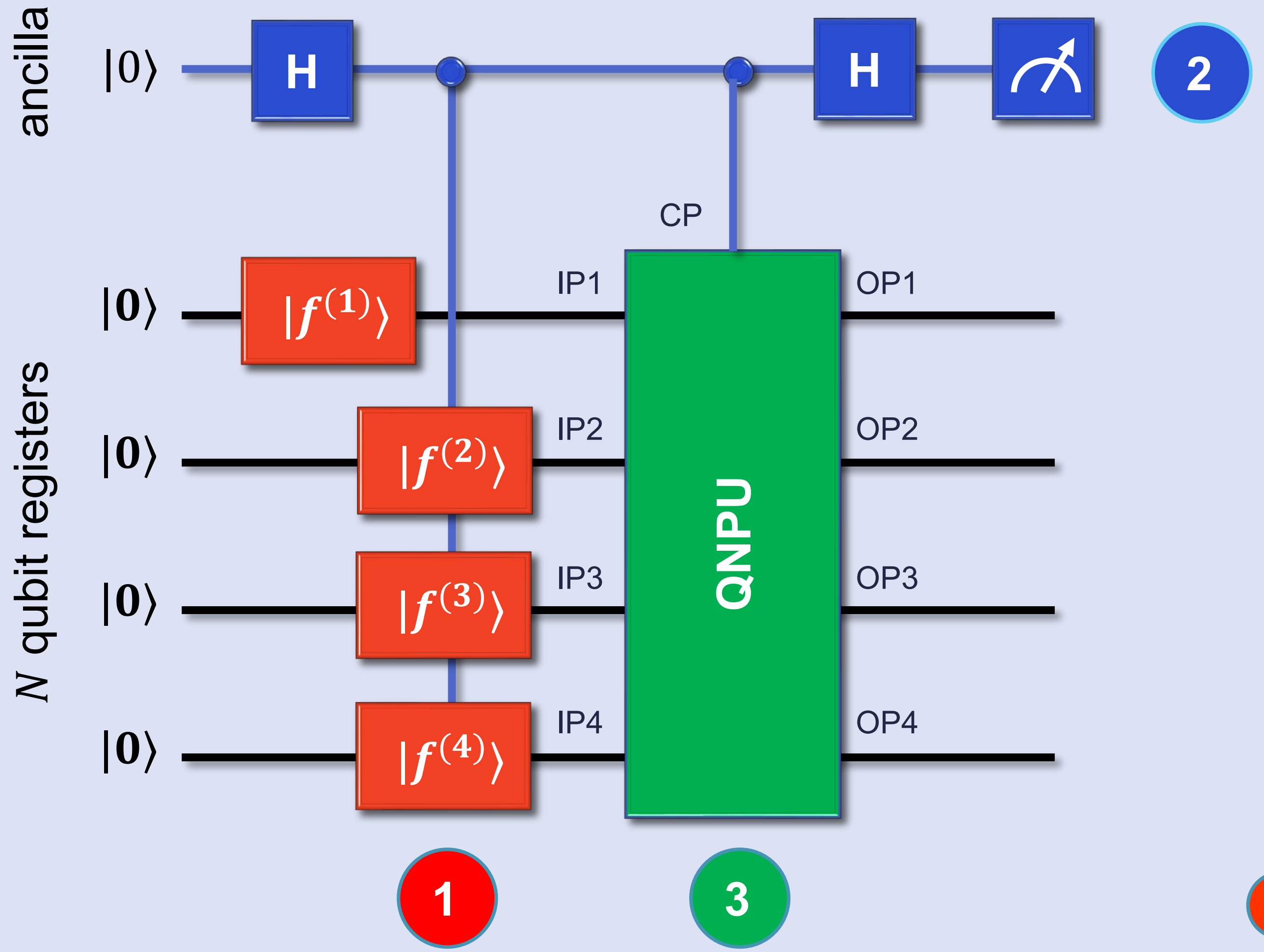

$$\mathcal{C} = f^{(1)^*} \prod_{j=1}^{r} \left(O_j f^{(j)} \right)$$

1. Prepare a variational state ($\propto n$)
2. Measure cost function via ancilla qubit
3. QNPU - evaluate the cost function ($\propto n$)

M. Lubasch, J. Joo, P. Moinier, M. Kiffner & DJ, Phys. Rev. A **101**, 010301(R) (2020).

Tensor networks as a quantum programming paradigm

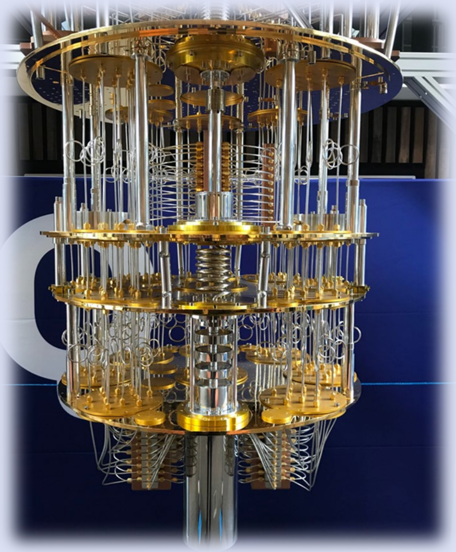

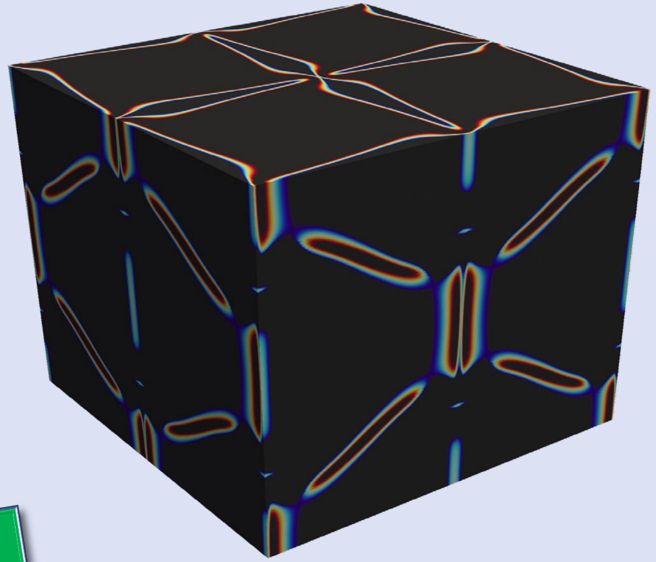

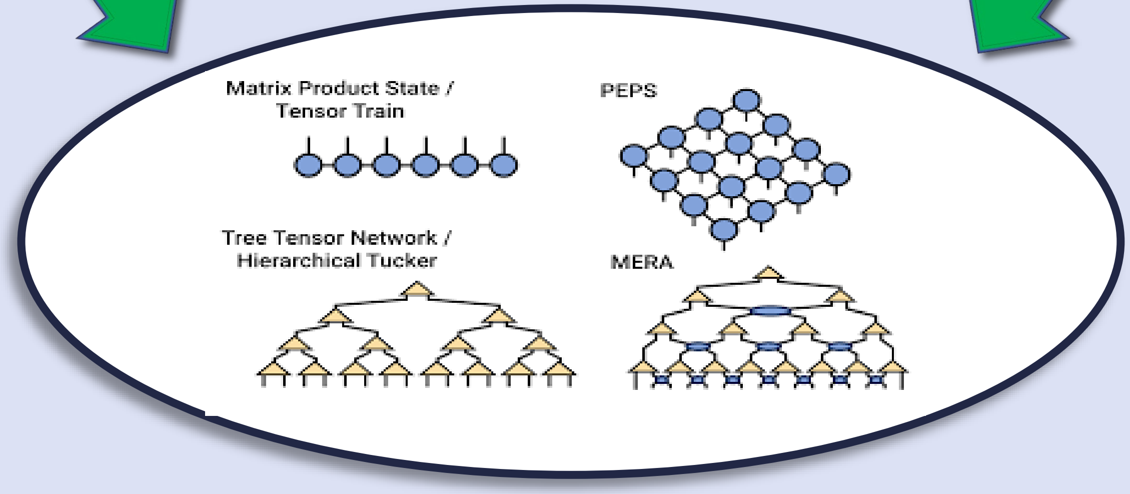

Variational quantum algorithms for computational fluid dynamics,
D Jaksch, P Givi, AJ Daley, T Rung
AIAA journal **61**, 1885 (2023)

❷ ❸ Modified Variational Quantum Algorithm

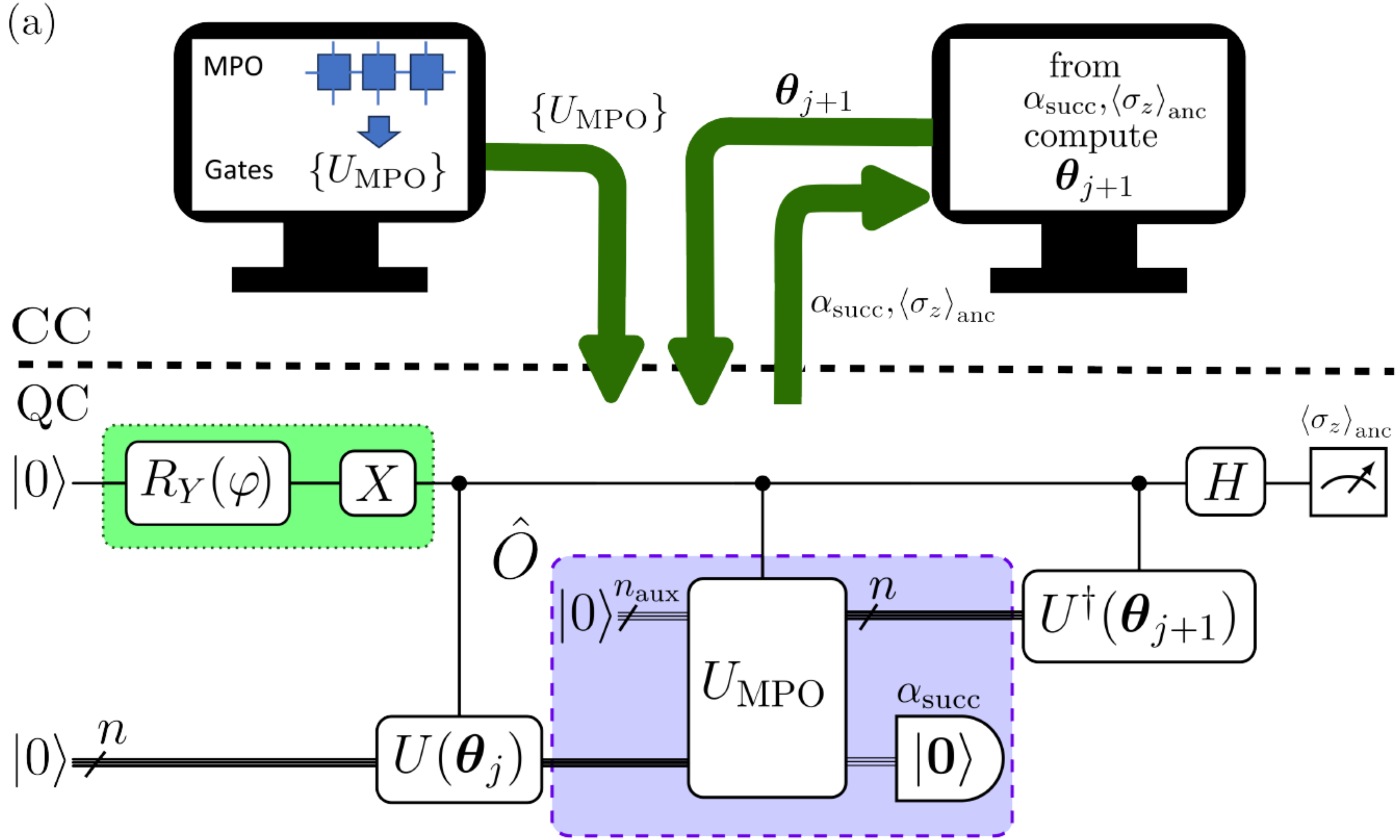

Termanova, et al., *Tensor quantum programming*, New J. Phys. **26**, 123019 (2024).

P. Siegl et al., Tensor-Programmable Quantum Circuits for Solving Differential Equations, arXiv:2502.04425.

Amplitude encoding of discrete functions

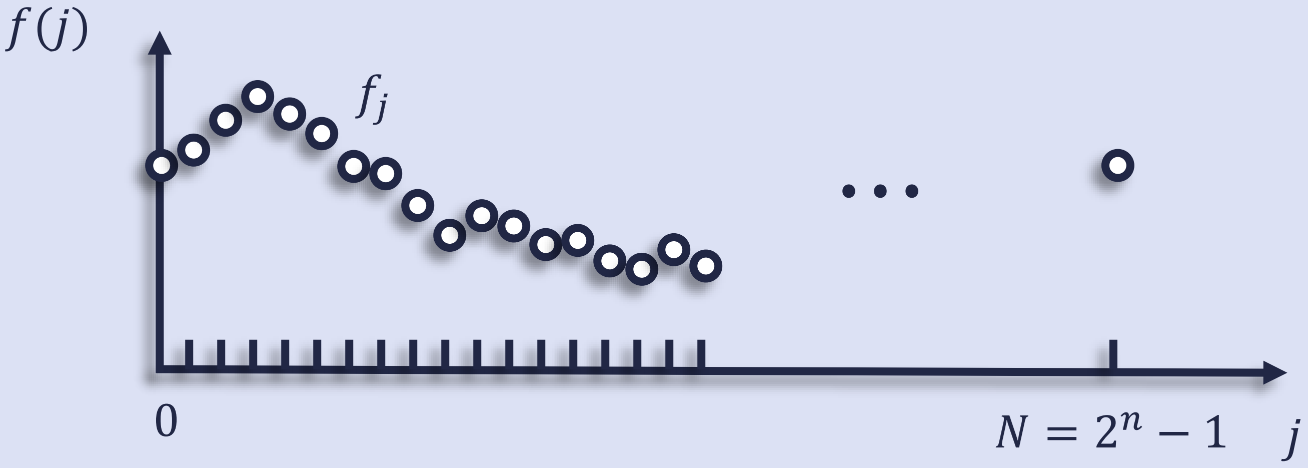

Quantum superposition

$$|\psi\rangle = \sum_i f_i |\vec{\imath}\rangle$$

n-qubit register stores 2^n function values f_j

Map $j \to \vec{\jmath} = \text{binary(j)}$ for $n = 8$:

$j = 0 \to \vec{\jmath} = 00000000$ $\quad$ $j = 1 \to \vec{\jmath} = 00000001$ $\quad$ $j = 2 \to \vec{\jmath} = 00000010$ $\quad$ ... $\quad$ $j = 255 \to \vec{\jmath} = 11111111$

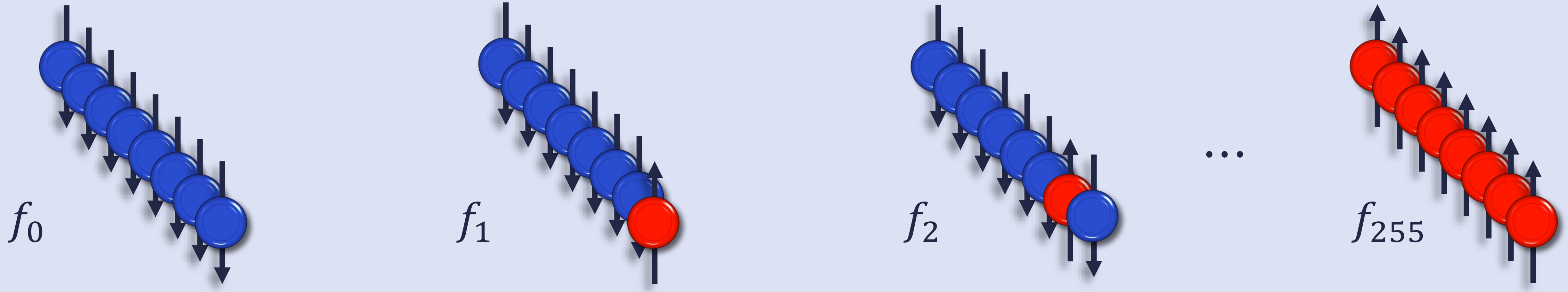

❶ Amplitude encoding of discrete functions

$f(j)$

Quantum superposition

n values f_j

Map j

$j = 0$

11111111

Function on a discrete grid of N

points requires $\log_2 N$ qubit registers

➔ guaranteed exponential memory saving compared to grid based methods

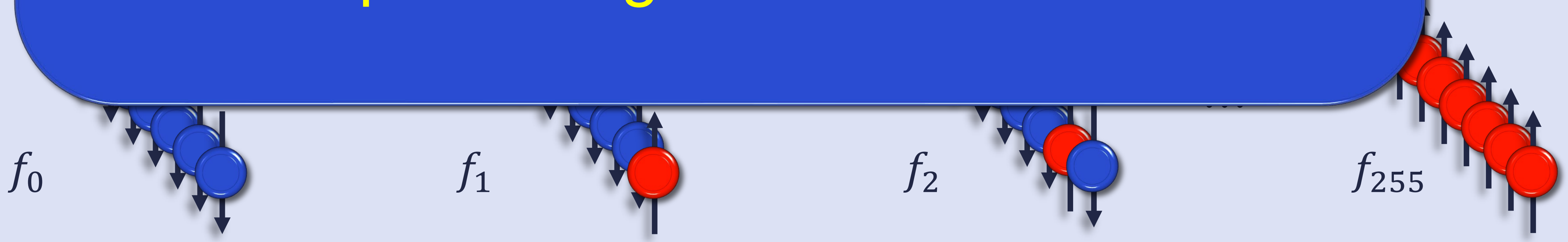

QCFD – required depth of the variational network

- Tensor Networks are a **programming paradigm** for quantum computers
  [Phys. Rev. A **101,** 010301(R) (2020)]

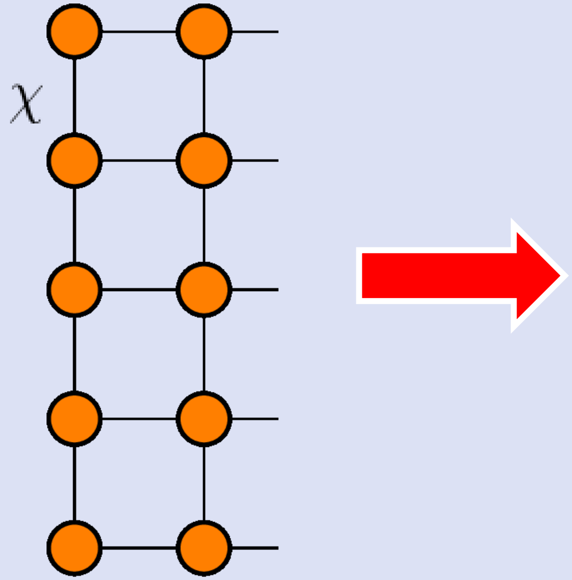

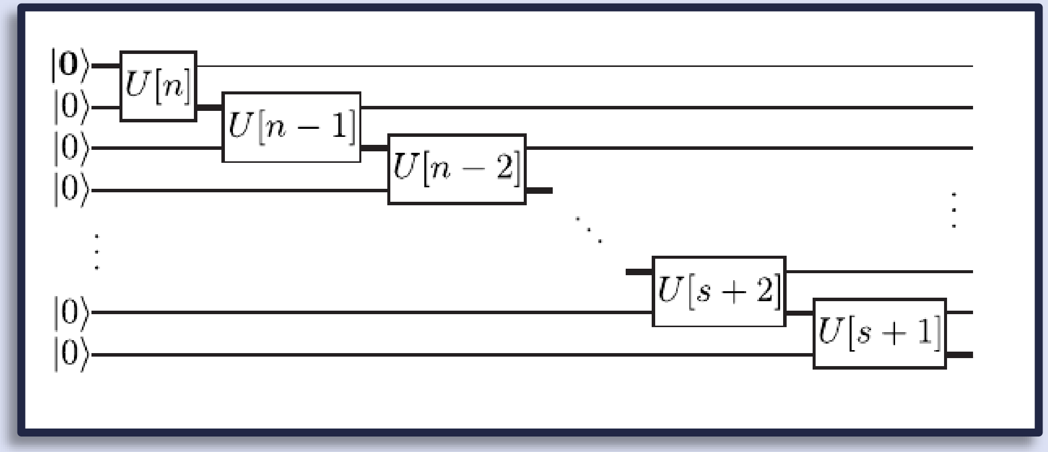

Classical complexity $\propto \chi^4$

Quantum complexity $\propto \chi^2$

- Quantum speed-up like in **Grover's algorithm**

QCFD – required depth of the variational network

- Tensor Networks are a **programming paradigm** for quantum computers
  [Phys. Rev

Classical circuit complexity $\propto \chi^4$

Quantum complexity $\propto \chi^2$

➔ guaranteed quadratic speedup over tensor network algorithms

Classic

- Quantum speed-up like in **Grover's algorithm**

QCFD – required depth of the variational network

- **Further possible quantum advantages**
  - **Systematic approach** via re-compilation of circuits
    [Quantum Sci. Technol. **5** 034015 (2020)]
  - Works entirely on quantum computers (work in progress)

- Problem-specific **quantum Ansatz**
  [Phys. Rev. A **101,** 010301(R) (2020)]

- **Exponential reduction** of variational parameters?

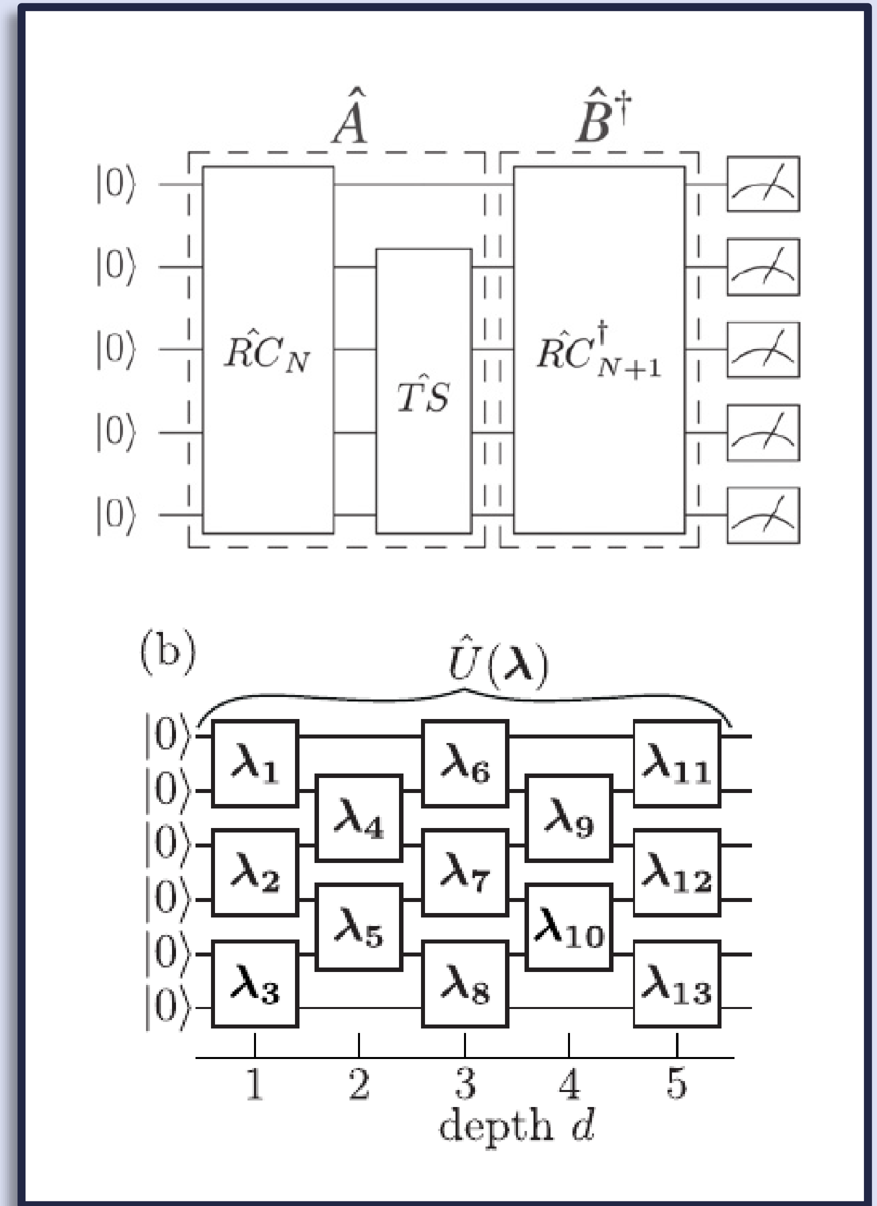

QCFD on actual quantum hardware - requirements

Burgers equation in 1D

$$\frac{\partial f}{\partial t} = \nu \frac{\partial^2 f}{\partial x^2} - f \frac{\partial f}{\partial x}$$

1D Burgers' equation requires 17 qubits in ideal computer

Porting the software to quantum hardware

- Platform optimized quantum circuits

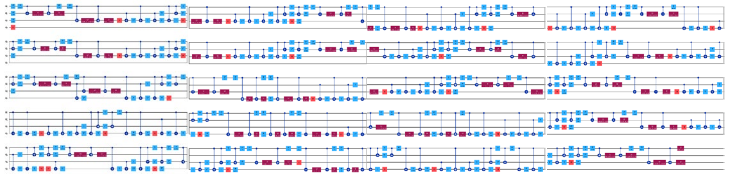

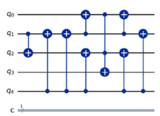

- Required quantum device and further optimizations

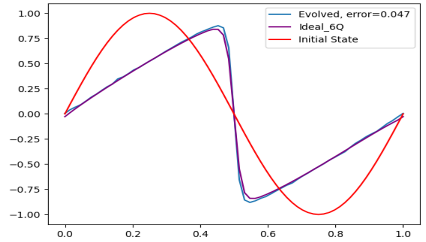

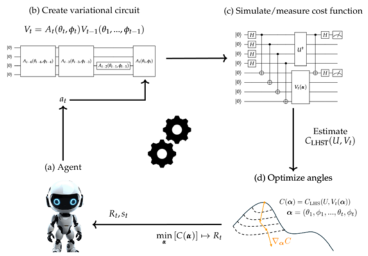

Gaining a quantum advantage in practice?

- Using our variational quantum algorithms:

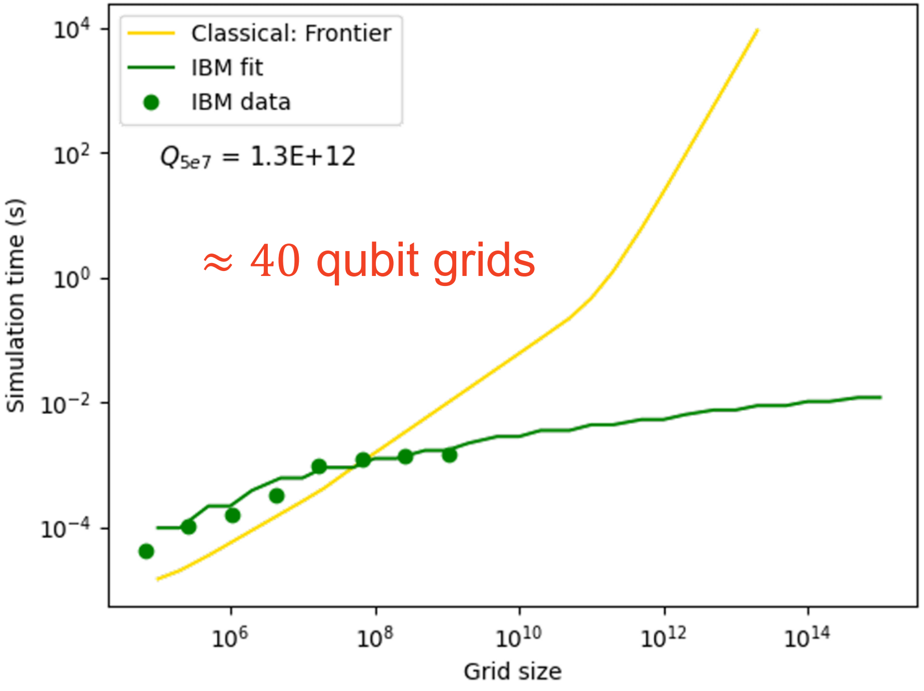

Computational Fluid Dynamics on Quantum Computers, arXiv:2406.18749

- Using HHL based linearized equation solvers

Flow past a sphere 10^{22} to 10^{28} T-gate calls

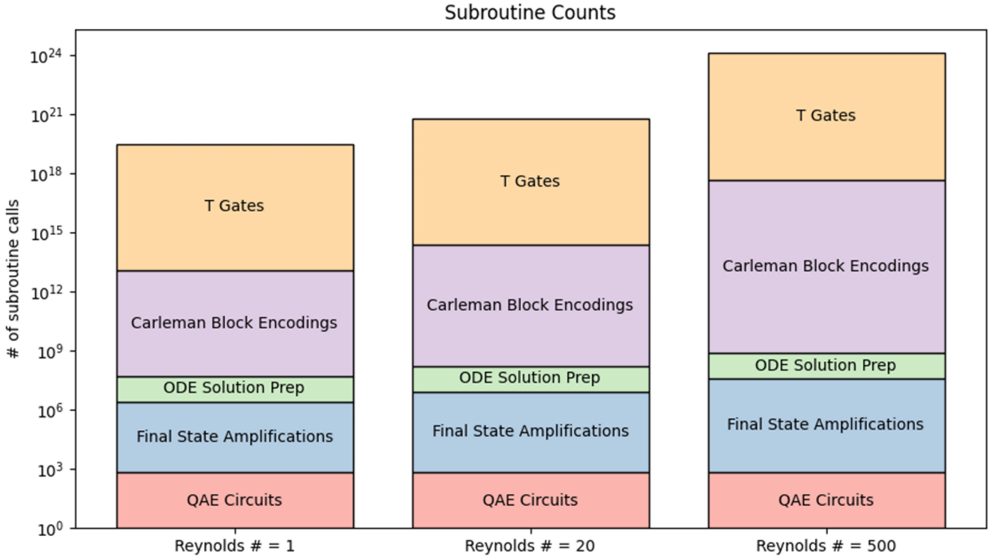

Feasibility of accelerating incompressible computational fluid dynamics simulations with fault-tolerant quantum computers, arxiv:2406.06323

The QCFD workflow

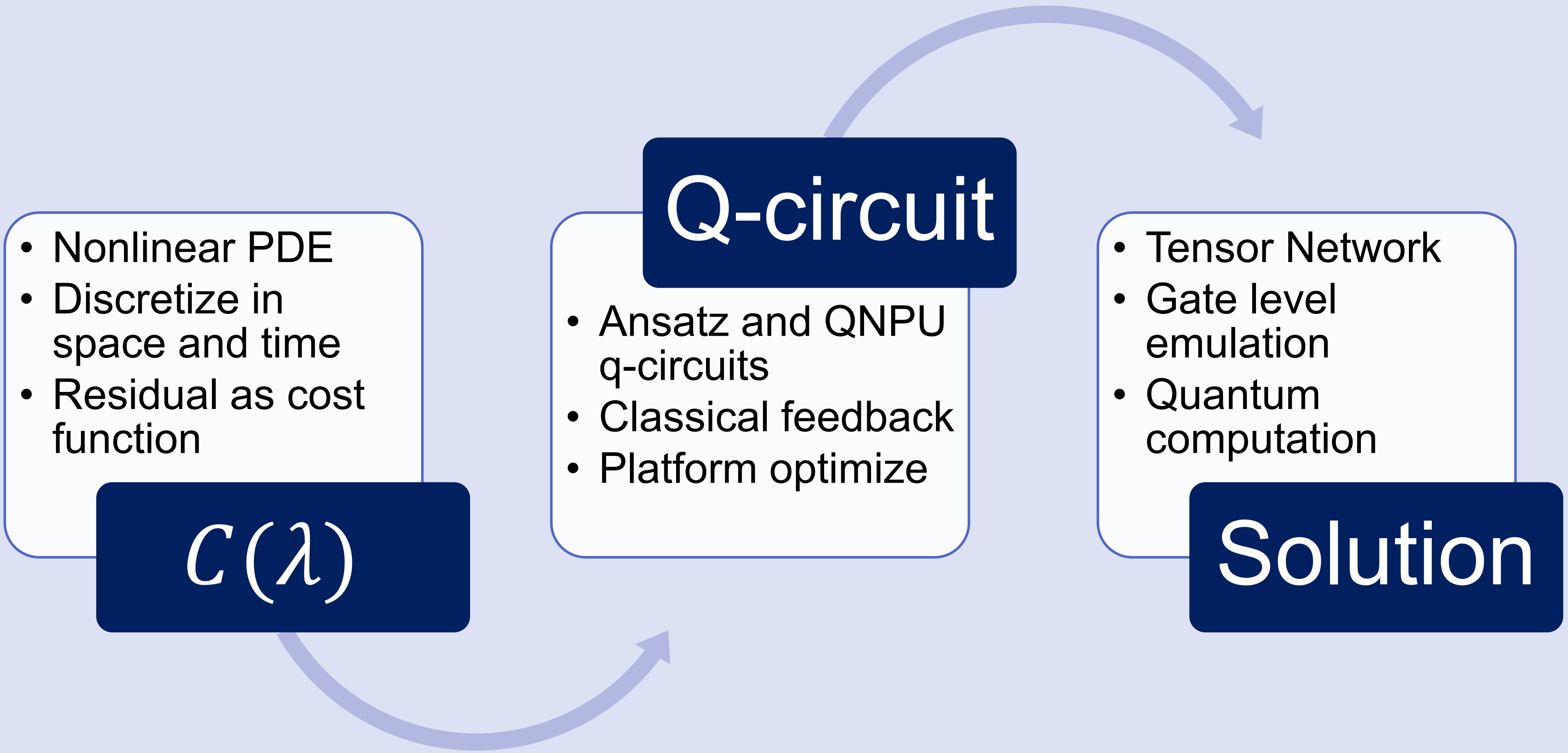

QCFD collaborations with hardware partners

2024

2025

2026

IBM Quantum

Low connectivity

QUANTINUUM

Low throughput

AQT

Improved throughput

TU Delft

Ok connectivity

IQM

Excellent connectivity

CHALMERS UNIVERSITY OF TECHNOLOGY

Good connectivity

OpenSuperQPlus

JÜLICH Forschungszentrum

Dedicated access

In-house optimization

QSOLID

planqc

Dedicated access

eleQtron

Improved throughput

PASQAL

Full controllability?

FZJ lead contact

QCFD consortium and collaborations beyond

Dieter Jaksch@UHH
Thomas Rung@TUHH
Felix Motzoi@Juelich
Barbara Kraus@TUM
Dimitris Angelakis@TUC
Paolo Geremia@ENGYS
Martin Kiffner@PlanQC

Steven@Cornell

Nik@OXF

Peyman@PIT

Michael@$\mathcal{Q}$

The QCFD project is funded under the EU's Horizon Programme (HORIZON-CL4-2021-DIGITAL-EMERGING-02-10), Grant Agreement 101080085.
QCFD (qcfd-h2020.eu)

AFOSR AIR FORCE OFFICE OF SCIENTIFIC RESEARCH
CUI THE HAMBURG CENTRE FOR ULTRAFAST IMAGING Advanced Imaging of Matter

Related publications

- **MPS encoding and Multigrid Renormalization**
  - M. Lubasch, P. Moinier and D. Jaksch, *Multigrid Renormalization,* J. Comp. Phys. **372**, 587 (2018)
- **Quantum Algorithms for nonlinear optimization**
  - M. Lubasch, J. Joo, P. Moinier, M. Kiffner and D. Jaksch, *Variational Quantum Algorithms for Nonlinear Problems,* Phys. Rev. A **101**, 010301(R) (2020)
- **QCFD and tensor network algorithms**
  - N. Gourianov, M. Lubasch, S. Dolgov, Q.Y. van den Berg, H. Babaee, P. Givi, M. Kiffner and D. Jaksch, *A quantum-inspired approach to exploit turbulence structures,* Nature Computational Science **2**, 30 (2022).
  - D. Jaksch, P. Givi, A.J. Daley and T. Rung, *Variational Quantum Algorithms for Computational Fluid Dynamics*, AIAA Journal **61**, 1885 (2023)
  - M. Kiffner and D. Jaksch, *Tensor network reduced order models for wall-bounded flows*, Phys. Rev. Fluids **8**, 124101 (2023)
  - P. Over, S. Bengoechea, T. Rung, F. Clerici, L. Scandurra, E. de Villiers, D. Jaksch, *Boundary treatment for variational quantum simulations of partial differential equations on quantum computers,* Computers & Fluids **288**, 106508 (2025)
  - N. Gourianov, P. Givi, D. Jaksch, and S.B. Pope, *Tensor networks enable the calculation of turbulence probability distributions*, Sci. Adv. **11**, eads5990 (2025)
  - S. Bengoechea, P. Over, D. Jaksch, and T. Rung, *Towards Variational Quantum Algorithms for generalized linear and nonlinear transport phenomena*, arXiv:2411.14931 (2024)
  - P. Siegl, G.S. Reese, T. Hashizume, N.-L. van Hülst, and D. Jaksch, *Tensor-Programmable Quantum Circuits for Solving Differential Equations*, arXiv:2502.04425 (2025)

QS